Cell Reports

Human labour pain is influenced by the voltage-gated potassium channel Kv6.4 subunit

--Manuscript Draft--

Manuscript Number:	CELL-REPORTS-D-20-01013R4
Full Title:	Human labour pain is influenced by the voltage-gated potassium channel Kv6.4 subunit
Article Type:	Research Article
Keywords:	pain; Labour; Quantitative Sensory Testing; Genetics; Nociceptors; Ion channels; electrophysiology; Immunohistochemistry
Corresponding Author:	Ewan Smith, MPharmacol, PhD University of Cambridge Cambridge, Cambridgeshire UNITED KINGDOM
First Author:	Michael Lee
Order of Authors:	Michael Lee
	Michael Nahorski
	James Hockley
	Van Lu
	Gill Ison
	Luke Pattison
	Gerard Callejo
	Kaitlin Stouffer
	Emily Fletcher
	Ichrak Drissi
	Daniel Wheeler
	Patrik Ernfors
	David Menon
	Frank Reimann
	Ewan Smith, MPharmacol, PhD
	Geoffrey Woods
Abstract:	By studying healthy women who do not request analgesia during their first delivery we investigate genetic effects on labour pain. Such women have normal sensory and psychometric test results, except for significantly higher cuff-pressure pain. We find an excess of heterozygotes carrying the rare allele of SNP rs140124801 in KCNG4 . The rare variant K V 6.4-Met419 exerts a dominant negative effect and cannot modulate the voltage-dependence of K V 2.1 inactivation because it fails to traffic to the plasma membrane. In vivo , Kcng4 (K V 6.4) expression occurs in 40% of retrograde labelled mouse uterine sensory neurones, all of which express K V 2.1, and over 90% express nociceptor genes Trpv1 and Scn10a . In neurones overexpressing K V 6.4-Met419, the voltage-dependence of inactivation for K V 2.1 is more depolarised compared to neurones overexpressing K V 6.4. Finally, K V 6.4-Met419 overexpressing neurones have a higher action potential threshold. We conclude that K V 6.4 can influence human labour pain by modulating the excitability of uterine nociceptors.
Suggested Reviewers:	Theodore Price Professor, University of Texas at Dallas theodore.price@utdallas.edu Basic scientist and expert in nociception and pain pathways. Employs molecular/

	cellular approaches
	Dave Bennett Professor (Neurologist), University of Oxford david.bennett@ndcn.ox.ac.uk Clinician Scientist; expertise in range of methods employed in our paper applied to neuropathic pain
	Frances Williams Professor, Twin Research and Genetic Epidemiology frances.williams@kcl.ac.uk Geneticist; interests in pain (clinical and neuro-biological perspectives)
	Brendan Carvalho Professor; Chief of Obstetric Anesthesia, Stanford University School of Medicine bcarvalho@stanford.edu Clinical researcher; expert in labour pain; obstetrics
Opposed Reviewers:	

Title

Human labour pain is influenced by the voltage-gated potassium channel $K_V6.4$ subunit.

Authors

Michael C. Lee[1*†], Michael S. Nahorski[2†] James R.F. Hockley[3†], Van B. Lu[4†], Gillian Ison[1], Luke A. Pattison[3], Gerard Callejo[3], Kaitlin Stouffer[2], Emily Fletcher[2], Christopher Brown[5], Ichrak Drissi[1], Daniel Wheeler[1], Patrik Ernfors[6], David Menon[1‡], Frank Reimann[4‡], Ewan St John Smith[3*‡#], C. Geoffrey Woods[2*‡]

Affiliations

1. University Division of Anaesthesia, University of Cambridge, Addenbrooke's Hospital, Hills Road, Cambridge CB2 0QQ, UK

2. Cambridge Institute for Medical Research, Wellcome Trust MRC Building, Addenbrooke's Hospital, Hills Rd, Cambridge CB2 0QQ, UK.

3. Department of Pharmacology, Tennis Court Road, Cambridge, CB2 1PD, UK

4. Wellcome Trust-MRC Institute of Metabolic Science, Addenbrooke's Hospital, Hills Road, Cambridge, CB2 0QQ, UK

5. Department of Psychological Sciences, Institute of Psychology, Health and Society, University of Liverpool, L69 7ZA

6. Department of Medical Biochemistry and Biophysics, Karolinska Institutet, SE-171 77 Stockholm, Sweden.

† These authors contributed equally to this paper. ‡ Joint senior authors

* Corresponding author(s)

Lead contact

Email address(es) of corresponding author(s)

Ewan St John Smith (es336@cam.ac.uk) – Lead contact

Michael C. Lee (ml404@cam.ac.uk)

Frank Reimann (fr222@cam.ac.uk)

C. Geoffrey Woods (cw347@cam.ac.uk)

ABSTRACT

By studying healthy women who do not request analgesia during their first delivery we investigate genetic effects on labour pain. Such women have normal sensory and psychometric test results, except for significantly higher cuff-pressure pain. We find an excess of heterozygotes carrying the rare allele of SNP rs140124801 in *KCNG4*. The rare variant K_V6.4-Met419 exerts a dominant negative effect and cannot modulate the voltage-dependence of K_V2.1 inactivation because it fails to traffic to the plasma membrane. *In vivo*, *Kcng4* (K_V6.4) expression occurs in 40% of retrograde labelled mouse uterine sensory neurones, all of which express K_V2.1, and over 90% express nociceptor genes *Trpv1* and *Scn10a*. In neurones overexpressing K_V6.4-Met419, the voltage-dependence of inactivation for K_V2.1 is more depolarised compared to neurones overexpressing K_V6.4. Finally, K_V6.4-Met419 overexpressing neurones have a higher action potential threshold. We conclude that K_V6.4 can influence human labour pain by modulating the excitability of uterine nociceptors.

Introduction

All eutherians (placental mammals) experience contraction of the uterus and discomfort during parturition. Whilst this discomfort is universal in eutherians, it appears to be most marked in humans (Maul, 2007). The severity of labour pain is considered a consequence of positive sexual selection in modern humans (with females seeking the cleverest mate), which has led to the human brain (and head) being three times the relative size of our nearest primate relatives (Sherwood et al., 2012). Despite neoteny (birth of offspring in a relatively immature state), this imposes a need to deliver a large neonatal head through the birth canal causing labour pain (Gruss and Schmitt, 2015). While labour pain is clearly linked to uterine contractions and cervical distension, the generation of this visceral signal and the sensory afferents involved are poorly understood (Labor and Maguire, 2008).

Although there are well-established ethnic, social and cultural factors that influence the experience and expression of pain during labour (Whitburn et al., 2017), broader genetic effects on labour pain may also exist. For example, women with the very rare Mendelian disorder Congenital Insensitivity to Pain due to bi-allelic non-functional mutations in *SCN9A* (OMIM: 243000) do not report labour pain or require analgesics during labour (Haestier et al., 2012). *SCN9A* encodes for the voltage-gated sodium channel $Na_V1.7$, expressed selectively in nociceptive and autonomic neurones, and mutations in *SCN9A* have well-documented roles in causing extremely painful or painless phenotypes (Bennett et al., 2019). The painlessness conferred by loss of function *SCN9A* mutations is clearly maladaptive and can be associated with severe injury during human parturition (Wheeler et al., 2014).

Our aim here was not to discover very rare Mendelian mutations that cause extreme painlessness, for example, congenital insensitivity to pain. Instead, the genetic analyses employed here are optimized for investigation of phenotypes that require both an environmental trigger and genetic predisposition, that will not appear to have a Mendelian inheritance pattern, unless the triggering event is frequent (Stouffer et al., 2017). This approach is suited to the study of labour pain, which may be considered nociceptive in nature, with parturition serving as visceral stimulus. We sought to identify functional SNP alleles that are over- or under-represented in a cohort of women who did not request or use analgesics that were available and offered to them during labour: an observable behavioural phenotype that is considered highly unusual in hospital maternity units in the United Kingdom, particularly for the spontaneous delivery of term nulliparous women. Quantitative sensory testing, performed with our study cohort, suggest a general increase in pain thresholds and tolerance when compared to controls, but only the increase in cuff-pressure pain threshold survived statistical significance after adjustment for multiple comparisons. We next assessed the allele frequencies of all (genome-wide) protein changing single nucleotide polymorphisms (SNPs) in these women compared to population frequencies. We found that the voltage-gated potassium channel (K_V) modifier *KCNG4* ($K_V6.4$) SNP rs140124801 rare allele c.1255G>A p.(Val419Met) was over-represented. Finally, we demonstrate effects of this rare $K_V6.4$-Met419 variant on sensory neurone excitability, and hence reveal a mechanism through which uterine nociception, and hence labour pain, can be attenuated in humans.

RESULTS

Identifying women who did not require analgesics during labour as nulliparous parturients: the test cohort

1029 potential cases were identified from 8 maternity units in the United Kingdom over a three-year period. Each potential case was invited to contact researchers, as chronologically ascertained. 383 women responded and were screened via telephone (Figure S1A). Key inclusion criteria were: healthy Caucasian women who experienced term (beyond 37-week gestation) and spontaneous vaginal delivery as nulliparous parturients without any use or request for any form of systemic or regional analgesia (spinal or epidural). We excluded women who had major disease or co-morbidities that are known to influence labour pain or pain in general. 189 women met the full eligibility criteria (Table S1), returned written consent, and donated either 10 ml of blood (collected at their local hospital) or 2 ml of saliva sent via post, from which DNA was extracted.

Of the women who donated DNA, 39 consented for a subsequent study of psychometrics and quantitative sensory testing. These women comprised a subset of the genetic discovery cohort for a case-controlled study (Figure S1B). For the control cohort, we recruited 33 women who were matched in age at delivery of the firstborn and location of maternity service, but who used analgesics during labour and delivery of their firstborn (Table S1). There were no significant differences in the means of new-born weight or head circumference between test and control cohorts (Table 1).

Cognitive and emotional function is normal in the test cohort

Psychometrics, comprising validated questionnaires and computerized cognitive assessments, were employed to quantify mood, beliefs and personality traits that can influence pain in experimental or clinical settings. The questionnaires included were: Hospital Anxiety and Depression Scale (HADS) (Zigmond and Snaith, 1983), Pain Catastrophizing Scale (PCS) (Sullivan et al., 1995), Multidimensional Health Locus of Control Scale (MHLC) (Stevens et al., 2011) and Life Orientation Test-Revised (LOTR) (Scheier et al., 1994). Computerized cognitive assessments were implemented in CANTAB® (Cambridge Cognition, UK) (Robbins et al., 1998). There were no significant differences in psychological or cognitive measures between control and test cohorts (Table S2).

Experimental pain thresholds and tolerance are increased in the test cohort

Next, we quantified sensory detection and pain thresholds to cold, heat and mechanical pressure. Thermal stimuli were delivered using a skin thermode applied to the forearm. Mechanical pressure was exerted via compression of upper arm by a sphygmomanometer cuff. There were no significant differences in the detection thresholds of cold or cuff-pressure in the test and control cohorts to suggest sensory deficits or impairments pertaining to those stimuli in the test cohort (Table 1, Figure S2A). Warmth detection thresholds

were very slightly but significantly lower in the test cohort compared to controls (0.54 °C difference) but all individual values fell within established norms for the general population (Rolke et al., 2006a).

The test cohort had increased pain thresholds to heat, cold and cuff-pressure compared to controls at an unadjusted significance level of $P<0.05$ (Figure S2A). There was a very striking increase of over 50 mmHg in the cuff-pressure pain threshold ($P = 0.00002$, uncorrected; $P = 0.00012$, Sidak's correction) (Table 1), suggesting that this characteristic might be relevant to the lack of analgesic requirement during nulliparous labour in the test cohort.

During testing for tolerance to pain from the immersion of hand in cold water (3 °C), when compared to controls, the test cohort showed increased hand withdrawal latency ($P = 0.03$, uncorrected), lower post-immersion skin temperatures ($P = 0.02$, uncorrected), and lower peak intensity of pain on the 100 mm Visual Analogue Scale (VAS) ($P = 0.004$, uncorrected; $P = 0.02$, Sidak's correction) on later assessment (Figure S2B). The Short-Form McGill Pain questionnaire (Melzack, 1987) revealed lower scores ($P = 0.01$, uncorrected; $P = 0.049$, corrected) for the sensory descriptors for the test group. There was no between-group difference in scores related to the affective aspects of the experimentally induced pain experienced ($P = 0.26$). These individual results do not survive statistical correction for multiple comparisons, further work is necessary to determine whether cold-pain tolerance differs between the test and control cohort.

The rare allele of rs140124801 in *KCNG4* is over-represented in the test cohort

In 158 of the 189 women who did not require analgesics during their first labour, we obtained enough high-quality DNA for molecular genetic analysis (Figure S1). The chronologically first 100 such women (by date of banking DNA) constituted a discovery cohort (Figure 1A); the next 58 women constituted our replication cohort. Those in the discovery cohort each had exome sequencing, from which we used the bam and bam.bai files for genome wide SNP allele frequency assessment using the fSNPd programme (Stouffer et al., 2017). The replication cohort of 58 were assessed only for SNP rs140124801 alleles using Sanger sequencing of genomic DNA.

Our discovery cohort analysis identified one ion channel SNP where the allele frequency was altered compared to reference (Figure 1A, Table S3). The rare allele of rs140124801 in *KCNG4* was over-represented, being found in 3 instances, whereas 0.7 instances were expected (q=<0.05, FDR corrected). We examined the individual exome results using the Integrated Genome Viewer (https://software.broadinstitute.org/software/igv/) and found that 3 individuals were heterozygous for the rare allele and confirmed this by Sanger sequencing. In the replication cohort, we found one further rare SNP rs140124801 heterozygote. For the total cohort of 158 women not requiring analgesia during their first delivery, there were 4 heterozygotes carrying the rs140124801 rare allele compared to an expected 1.1 (Chi-squared two tail with Yates correction = 4.779, $P = 0.0288$; Figure S1A).

In case-controlled studies, we further explored whether 3 of the individuals who possess the rare *KCNG4* allele had significantly different experimental pain thresholds to those who did not (n=69, Figure S1B). We

investigated pain thresholds for heat, cold and cuff-pressure, and found that the rare *KCNG4* allele was associated with a significantly increased cuff-pressure pain threshold ($P = 0.0029$, uncorrected; $P = 0.009$, Sidak's correction, Table S4). Although the sample size here is very small because of the rarity of the *KCNG4* allele being examined, the finding suggests that an effect of this rare-allele is to increase experimental cuff-pressure pain threshold in humans. The experimental cuff-pressure pain remains significantly increased in the test cohort (even with the 3 rare-allele cases excluded, when compared with the control group ($P = 0.0029$, uncorrected; $P = 0.009$, Sidak's correction, Table S4) suggesting that cuff-pressure pain threshold might be relevant to the labour pain. Whilst, there are clearly other reasons for increased cuff-pressure pain threshold in those cases who do not carry the rare *KCNG4* allele, these data suggest that the rare-allele of *KCNG4* may be related to the lack of analgesic requirement for the 3 cases we identified in this study.

The p.Val419Met change in K_V6.4 impairs function of K_V2.1 heterotetramers

The rare allele of rs140124801 in *KCNG4* causes the mis-sense change p.Val419Met encoding the voltage-gated potassium channel K_V6.4 (from here on referred to as K_V6.4-Met419; Figure 1A-B). Voltage-gated potassium channels are tetrameric complexes with each subunit having six transmembrane domains (S1-S6). K_V6.4 is a member of the electrically silent group of K_V subunits, which cannot form functional plasma membrane-expressed homotetramers, but instead act as modulators of K_V2 subunits (Bocksteins and Snyders, 2012). Indeed, K_V6.4 is known to heterotetramerise with K_V2.1 in a 1:3 stoichiometry (Bocksteins et al., 2017). Valine 419 is in the pore forming S5-S6 linker and is part of the highly conserved K^+ selectivity filter consensus sequence (T**V**GYG) (Figure 1C), in which the equivalent position is always occupied by a branched chain amino acid. Whilst originally thought to be relatively rigid, this structure is also involved in open-pore or C-type inactivation, as subtle rearrangements block the conductive path of K^+ ions (Cuello et al., 2010). It therefore seemed likely that rs140124801 might affect K^+-selectivity and/or inactivation and thus we studied the electrophysiological properties of K_V6.4-Met419 in complex with K_V2.1 compared to the most frequent *KCNG4* allele that possesses a valine at position 419 (K_V6.4) in complex with K_V2.1.

We used HEK293 cells as a heterologous expression system that does not express significant endogenous K_V currents (Figure S3). As expected, over-expression of K_V6.4 or K_V6.4-Met419 alone did not produce measurable K^+ currents (Figure S3E). However, in cells expressing K_V2.1 alone, outward currents were observed that were activated by potentials more positive than −40 mV and displayed a slow inactivation (Figure S3A). Co-expression of K_V2.1 with K_V6.4 produced outward currents with similar kinetics (Figure S3D), but we observed a small shift in the voltage of half-maximal activation ($V_{0.5}$ act) to more negative potentials. This shift was not observed when K_V6.4-Met419 was co-expressed with K_V2.1 (Figure S3D). The current amplitude generated was similar between wild-type K_V6.4 or K_V6.4-Met419 co-expressed with K_V2.1 (Figure S3E) showing that expression of K_V6.4-Met419 does not negatively regulate maximal current

flux, over wild-type $K_V6.4$, a factor that would impact sensory neurone excitability (Figure S3E). The slope factors of the Boltzmann fits did not significantly differ between the 3 groups ($K_V2.1$: k = 9.5 ± 0.8, n = 13; $K_V2.1$ + $K_V6.4$: k = 15.9 ± 1.7, n = 14; $K_V2.1$ + $K_V6.4$-Met419: k = 11.0 ± 0.8, n = 13; one-way ANOVA, P > 0.05). Furthermore, the reversal potential was not significantly different between the groups (Figure S3F).

Similar to previous reports (Bocksteins et al., 2012), co-expression of $K_V6.4$ resulted in a large hyperpolarising shift in the voltage-dependence of inactivation by ~30 mV compared to $K_V2.1$ homomeric currents (Figure 1D, E & G). This hyperpolarising shift was not observed when $K_V2.1$ was co-expressed with $K_V6.4$-Met419 (Figure 1F & G). There was however no significant difference in the slope factor of inactivation curves between the three groups ($K_V2.1$: k = 9.8 ± 1.4, n = 9; $K_V2.1$ + $K_V6.4$: k = 13.6 ± 2.4, n = 12; $K_V2.1$ + $K_V6.4$-Met419: k = 12.2 ± 1.2, n = 15; Kruskal-Wallis, $P > 0.7$), or in their time courses of recovery from inactivation (Figure S3G). These data suggest a loss of $K_V6.4$ function as a result of the p.Val419Met mutation.

$K_V6.4$-Met419 does not traffic with $K_V2.1$ to the plasma membrane

As discussed above, $K_V6.4$ forms heterotetramers with $K_V2.1$ with altered biophysical properties compared to homotetrameric $K_V2.1$ channels (Bocksteins, 2016) (Figure 1D-G, Figure S3). In addition, $K_V6.4$ is retained in the endoplasmic reticulum in the absence of $K_V2.1$, requiring the expression of $K_V2.1$ for trafficking to the cell membrane (Ottschytsch et al., 2005). We thus tested whether the p.Val419Met alteration might affect the trafficking of $K_V6.4$. For this, $K_V6.4$ was cloned into a pcDNA3 based vector containing a CMV-polioIRESmCherry expression cassette, tagged with HA and the p.Val419Met alteration introduced. $K_V2.1$ had been previously cloned into the pCAGGS-IRES2-nucEGFP which displays nuclear GFP signal upon transfection. To assess membrane localisation, HEK293 cells were co-transfected with both $K_V2.1$ and $K_V6.4$, stained for HA-tagged $K_V6.4$, with co-expressing cells identified by both mCherry and nuclear GFP signal. $K_V6.4$ was retained within the cytoplasm in the absence of $K_V2.1$ expression but displayed a striking shift to the cell membrane upon co-transfection with $K_V2.1$ (Figure 2A). There was no appreciable difference in the localization of $K_V6.4$-Met419 in the absence of $K_V2.1$, but in the presence of $K_V2.1$ and in contrast to the wild-type protein, $K_V6.4$-Met419 was retained intracellularly and showed no membrane localization (Figure 2A). Importantly, expression of $K_V6.4$-Met419 in HEK293 cells showed only a modest reduction in steady-state stability compared with wild-type $K_V6.4$, and this was not affected by co-expression with $K_V2.1$ (Figure 2B-C).

$K_V6.4$ is expressed in nociceptors that innervate the uterus

Altered K_V function produces dramatic effects upon sensory neurone excitability; K_V7 openers (Peiris et al., 2017) and K_V2 inhibitors (Tsantoulas et al., 2014) decrease and increase sensory neurone excitability respectively. We hypothesised that expression of $K_V6.4$-Met419 within sensory neurones innervating the uterus would alter neuronal excitability and contribute to the impaired nociception. We first investigated the expression of *Kcng4* and *Kcnb1* in mouse uterine sensory neurones using single-cell qRT-PCR of sensory

neurones retrogradely labelled with fast blue from the uterus (Figure 3A). Sensory innervation of the mouse uterus possesses two distinct peak densities within thoracolumbar (TL) and lumbosacral (LS) spinal segments (Herweijer et al., 2014). As such, fast blue-positive uterine sensory neurones were collected from dorsal root ganglia (DRG) isolated from vertebrae levels T12-L2 and L5-S2. These had an average cell diameter of 31.0 ± 0.7 µm (n = 89), which is in broad agreement with studies investigating sensory neurones innervating the uterus and other visceral organs including the distal colon (Herweijer et al., 2014; Hockley et al., 2019). Most uterine neurones expressed *Kcnb1* (TL: 82% [36/44] and LS: 66% [30/45]) and *Kcng4* mRNA was detected in a subset of uterine neurones from both spinal pathways (TL: 43% [19/44] and LS: 24% [11/45]; Figure 3B). The average cycle threshold (CT) value for *Kcng4* expressing neurones was higher than that of *Kcnb1* (27.2 vs. 16.3, Figure S4), which may indicate relative lower expression levels. Importantly, all but one LS neuron co-expressed *Kcng4* with *Kcnb1*, suggesting that these two K_V subunits are predominantly present in the same uterine sensory neurone subset. We also assessed the mRNA expression of the nociceptor markers transient receptor potential vanilloid 1 (*Trpv1*) and voltage-gated sodium channel 1.8 (S*cn10a*). In *Kcng4*-positive uterine sensory neurones *Trpv1* mRNA was present in 100 % of TL and 91 % of LS neurones, and *Scn10a* in 95 % of TL and 91 % of LS neurones, suggesting that K_V6.4 is expressed by a population of neurones capable of transducing noxious stimuli. (Figure 3B).

K_V6.4–Met419 causes loss of modulatory function of K_V2.1 and decreases neuronal excitability in DRG sensory neurones

Given the high co-expression of *Kcng4* with *Kcnb1* in uterine sensory neurones, we next characterized the effect of K_V6.4 and K_V6.4–Met419 on sensory neuronal function. We recorded outward delayed rectifier K^+ currents (I_K) and investigated the effect of transient transfection of either K_V6.4 or K_V6.4-Met419 on the stromatoxin-1(ScTx)-sensitive I_K; ScTx is a gating modifier of K_V2.1, K_V2.2 and K_V4.2 which effectively blocks these channels (Escoubas et al., 2002), as well as K_V2.1 heterotetramers formed with silent K_V subunits (Zhong et al., 2010). Through subtraction of I_K in the presence of ScTx from the total I_K in the absence of ScTx, we isolated the ScTx-sensitive I_K, which is predominantly dependent on K_V2 channels (Figure 3C-F). A diverse and heterogenous population of K_V2 and silent K_V subunits is expressed in sensory neurones (Bocksteins et al., 2009; Hockley et al., 2019; Zeisel et al., 2018) and previous studies suggest that silent K_V subunits only heterotetramerise with K_V2 subunits and not K_V1, K_V3 and K_V4 subunits (Bocksteins, 2016). As such, we predicted that wild-type K_V6.4 heterotetramerisation with K_V2.1 in sensory neurones would produce functional channels, but with a hyperpolarised shift in the voltage-dependence of inactivation compared to homotetrameric K_V2.1 channels, as we (Figure 1D-G) and others have observed previously in HEK293 cells (Bocksteins, 2016). By contrast, we hypothesised that the K_V6.4-Met419 subunit would be unable to evoke such a hyperpolarising shift in the voltage-dependence of inactivation.

By transfecting mouse sensory neurones with either K_V6.4 or K_V6.4-Met419, we attempted to bias available K_V2.1 into heterotetramers with K_V6.4 subunits, thus increasing the probability of recording the contribution of K_V2.1/K_V6.4 heterotetramers to ScTx-sensitive I_K. In both K_V6.4 and K_V6.4-Met419 experiments,

addition of ScTx led to a maximum reduction in the outward K^+ current at a 20 mV step potential, which did not differ significantly (K_V6.4, 52.7 ± 3.8 %; K_V6.4-Met419, 45.1 ± 7.7 %; Student's t-test, $P = 0.37$; Figure 3C-E). The voltage-dependence of ScTx-sensitive I_K activation was similar for neurones transfected with K_V6.4 or K_V6.4-Met419 subunit ($V_{1/2}$ = −5.4 ± 1.8 mV *vs.* −9.8 ± 1.1 mV, and k = 8.6 ± 1.5 *vs.* 8.9 ± 0.9, respectively; Figure S5). As observed previously (Bocksteins et al., 2009), the voltage-dependence of ScTx-sensitive I_K inactivation, for both K_V6.4 and K_V6.4-Met419 experiments, was multifactorial and fitted with a sum of two Boltzmann functions. In neurones transfected with K_V6.4, the midpoint of the first component was −0.8 ± 29.5 mV, which likely correlates with homotetrameric K_V2.1 currents. The second component possessed a midpoint of inactivation of −60.2 ± 6.6 mV (n = 8); a current that is likely a function of heterotetrameric K_V2/silent K_V channels or differentially phosphorylated K_V2 channels and in line with what others have reported for the second component of I_K in DRG neurones in the presence of ScTx (Bocksteins et al., 2009). Importantly, expression of K_V6.4-Met419 led to a significant depolarising shift in the second component of the voltage-dependence of inactivation (−33.8 ± 2.1 mV, n = 7, unpaired t-test, $P = 0.003$, Figure 3F), whilst the first component, attributed to homotetrameric K_V2.1 I_K, remained unchanged (-36.2 ± 3.3 mV, unpaired t-test, $P = 0.29$, Table S5A).

We assessed the functional consequences on neuronal excitability of such a shift in the availability of K_V2 channels towards more depolarised potentials through current clamp experiments. The threshold for action potential discharge was assessed for neurones transfected with either K_V6.4 or K_V6.4-Met419, as well as neurones which exhibited no mCherry fluorescence from cultures exposed to either plasmid (considered untransfected). Neurones transfected with K_V6.4-Met419 exhibited a higher threshold, than those overexpressing K_V6.4 or untransfected neurones during injection of a progressively depolarising current, (ramp protocol: 0-1 nA, 1s), however, only the difference between K_V6.4-Met419 and K_V6.4 reached statistical significance (K_V6.4, 91.6 ± 16.7 pA *vs.* K_V6.4-Met419, 248.6 ± 50.3 pA, ANOVA with Bonferroni multiple comparisons $P = 0.018$; Untran., 112.5 ± 32.5 pA *vs.* K_V6.4-Met419 248.6 ± 50.3 pA, $P = 0.087$; Figure 3G-H). A higher current was also required to evoke action potentials when threshold was assessed with a step protocol (+10 pA, 50 ms injections, starting at 0 pA). Similarly, only the difference between K_V6.4 and K_V6.4-Met419 proved significant (K_V6.4, 61.1 ± 12.2 pA *vs.* K_V6.4-Met419, 172.0 ± 34.4 pA, ANOVA with Bonferroni multiple comparisons $P = 0.012$; Untran., 88.3 ± 13.8 pA *vs.* K_V6.4-Met419 172.0 ± 34.4 pA, $P = 0.124$; Figure 3I). The ability of neurones to respond to capsaicin was also examined to identify putative nociceptors (i.e. those expressing *Trpv1*), but no obvious pattern regarding the subpopulations of nociceptive and non-nociceptive neurones within each group could be observed. Analyses of other action potential parameters revealed no further differences between neurones transfected with either K_V6.4 construct or untransfected cells (Table S5B). Taken together, these findings demonstrate that sensory neurones expressing K_V6.4-Met419 are less excitable than those transfected with the K_V6.4. We thus postulate that uterine primary afferent input into the pain pathway is likely to be reduced in women carrying the rare *KCNG4* SNP rs140124801 allele.

Heterozygous K_V6.4-Met419 acts as a dominant negative mutation to abolish wild-type function.

The SNP rs140124801 minor allele identified in those healthy women not requiring analgesia during their first labour was always in a heterozygote state. We asked if this heterozygous state has as much of an effect on K_V2.1 as the homozygous state used in our sub-cellular localisation and electrophysiology studies, or if the effect size was in-between homozygous K_V6.4 and homozygous K_V6.4-Met419. Indeed, our findings of reduced labour pain are compatible with the minor allele of rs140124801 having a dominant-negative effect, or a reduced dosage effect, but incompatible if acting as a recessive. K_V2.1 was co-transfected into HEK293 cells with equimolar concentration of K_V6.4 and K_V6.4-Met419, stained for HA-K_V6.4 and the membrane marker Na^+/K^+ ATPase. We found significant co-localisation of K_V6.4 with Na^+/K^+ ATPase at the plasma membrane, but no evidence of trafficking to the cell membrane for either homozygote K_V6.4-Met419, nor when K_V6.4 and K_V6.4-Met419 were co-transfected (Figure 4A-B).

Similarly, co-transfection of equimolar K_V6.4 and K_V6.4-Met419 with K_V2.1 produces electrophysiological properties comparable to transfection of K_V2.1 only, i.e. the co-expression of the minor allele variant prevented the hyperpolarising shift of the voltage-dependence of inactivation produced by the major allele variant (Figure 4C).

In addition, we investigated whether K_V6.4-Met419 might affect heterotetramerisation with K_V2.1. Co-immunoprecipitation experiments in transfected HEK293 cells demonstrate that, unlike K_V6.4, K_V6.4-Met419 is unable to bind to K_V2.1 (Figure S6A and S6B). When K_V6.4 is tagged but co-expressed with K_V6.4-Met419 (untagged), there is notably reduced binding of K_V6.4 to K_V2.1 (Figure 5A). Similarly, by immunofluorescence analysis, the presence of untagged K_V6.4-Met419 suffices to disrupt K_V6.4 trafficking to the plasma membrane (Figure 5B and 5C).

We therefore conclude that the K_V6.4-Met419 variant acts as a dominant negative subunit and significantly affects the function of K_V6.4 (and hence in turn K_V2.1) in the heterozygote state identified in our cohort of women who did not require analgesia during their first labour

DISCUSSION

Parturition may be physiological and widely considered to be 'natural' but remains amongst the most painful events in life that women can experience (Melzack, 1984). Labour pain is a complex experience with many biopsychosocial determinants, of which visceral nociception is fundamental and necessary. Although the cellular and molecular substrates for visceral nociception are ill defined in humans, ion channels that are important regulators of uterine sensory neurone excitability, may determine visceral nociception and hence labour pain.

Labour pain is challenging, if not impossible, to model adequately in pre-clinical laboratories. Our genetic approach in humans here was not to discover very rare Mendelian mutations that cause extreme and hence, pathological painlessness (e.g. Congenital Insensitivity to Pain). Instead, we sought to investigate SNPs that are more common, and for which frequencies in the general population are known. We hypothesised that such SNPs would be significantly over- or under-presented in a cohort of women with a less extreme, but nonetheless clinically relevant phenotype. Hence, we chose to investigate healthy nulliparous women who chose and were able to manage pain from spontaneous and uncomplicated vaginal delivery of term labour without any analgesia. In this group, there were no deficits in detection of innocuous warmth, cool or cuff-grip pressure to suggest clinically relevant sensory neuropathy. There were also no differences in cognitive test battery performance, pain-relevant personality traits or emotional function, when compared to controls. However, these women demonstrate increased pain and tolerance thresholds to a range of noxious stimuli, and significantly so for cuff-pressure pain.

Given that our painlessness phenotype is far less extreme compared to that of congenital insensitivity to pain, we did not expect that any rare-SNP(s) discovered in this study would cause a large increase in experimental pain threshold or tolerance for all stimulus modalities. Nonetheless, there is modest evidence from a study by Carvalho and colleagues that a composite of these measures obtained just before induction of labour in singleton, term pregnancies, predicts analgesic consumption, i.e. volume of local anaesthetic infused, in women who requested an epidural (Carvalho et al., 2013). We found that cuff-pressure pain threshold was robustly and very significantly increased in women who did not request any analgesic. Labour pain has visceral and somatic components, caused by contractions of uterine viscus, but also by sustained stretch or compression of pelvic floor, perineum and vagina (Labor and Maguire, 2008), which occur in the later stages of labour as the foetus descends, and may be experienced as a continuous background pain on which rhythmic pain caused by uterine contractions is superimposed (Melzack and Schaffelberg, 1987). Whilst speculative, the hypothesis that women with high cuff-pressure pain thresholds would report reduced intensity of continuous background pain during labour is testable.

Blinding was not feasible in our experiments and social desirability bias may explain our overall findings of increased threshold and tolerance of pain. However, such bias might be expected to also significantly lower scores for self-reported pain related traits, particularly pain catastrophizing (Sullivan et al., 1995), but that was not observed. Our data are consistent with those from other investigators who show that scores from

Pain Catastrophizing Scale and Fear of Pain questionnaires do not influence self-reported or behavioural measures of labour pain (Carvalho et al., 2014). Pain is a complex experience, with sensory-discriminatory and affective-motivational aspects (Loeser and Treede, 2008). We found that the test cohort had lower SFMPQ scores that pertained to the sensory, but not the affective qualities of the pain that was experienced during cold tolerance testing. In sum, we found increased threshold to pain from noxious stimuli (significantly so for cuff pressure), but no differences in cognitive, personality traits and emotional function, in women who did not require analgesics during term nulliparous labour. These findings suggest that nociceptive function is altered in these women and validate their selection to discover predisposing genetic changes in sensory neurones (nociceptors) that might influence labour pain in women: a phenotype that otherwise would confidently have been expected to be highly heterogeneous.

We detected a single SNP, rs140124801 in the gene *KCNG4* where the rare allele had a significant over-representation when compared to the general population in a cohort of 158 women who had no analgesic requirement during nulliparous labour, noting that ideally control allele frequencies would have been generated from a matched cohort of women who did require analgesia. There were 4 heterozygotes who possess the rare allele, and data on quantitative sensory and pain testing were available for 3 heterozygotes. We found that women who possess the rare allele showed a significantly increased cuff-pressure pain threshold, when compared to controls (Table S4). The rare allele of SNP rs140124801 causes a mis-sense change p.Val419Met in K_V6.4, a silent K_V subunit that forms heterotetramers with K_V2 channels and modulates their function (Bocksteins et al., 2012). We, and others, show that K_V6.4 traffics to the plasma membrane only when co-expressed with K_V2.1 (Ottschytsch et al., 2005). In contrast, we found that the rare allele product K_V6.4-Met419 failed to traffic to the plasma membrane when co-expressed with K_V2.1. Moreover, K_V6.4-Met419 failed to induce the hyperpolarising shift in the voltage-dependence of K_V2.1 inactivation that is observed with K_V6.4, likely indicating that the observed currents would be conducted by K_V2.1 homotetrameric channels.

We have found that K_V6.4-Met419 was unable to heterotetramerise with K_V2.1. A possible explanation for this is gained from X-ray crystallography of K_V2.1 homotetramer (RCSB Protein Data Bank ID: 3LNM; and see Supplemental data). Each of the four K_V2.1 monomers contributes equally to the K^+ ion selectivity region, which is formed by the peptide backbone carbonyl groups of the amino acids TVGYG. The side chains of Valine and Tyrosine from each of the four monomers fits within an aliphatic pocket of the adjacent monomer (composed of amino acids WWAIIS, see Figure 1C). The rare allele of SNP, rs140124801 results in Valine being changed to Methionine, the side chain of which is too large to be accommodated by this aliphatic pocket. This may be sufficient to stop K_V6.4 forming a heterotetramer with K_V2.1 and would be predicted to disrupt the close packing of the peptide backbone carbonyl groups of the ion selectivity region.

For K_V6.4 to modulate labour pain it needs to be expressed in an appropriate part of the sensory nervous system. We focused on uterine sensory neurones, but this does not negate the possibility that K_V6.4 also exerts influence elsewhere in the nervous system, *KCNG4* mRNA also being expressed in regions of the

spinal cord and brain (Figure S6C). We observed $K_V6.4$ expression in Trpv1 and $Na_V1.8$-positive mouse uterine sensory neurones, consistent with the observation that sensory neurones innervating deep tissues display comparatively high Trpv1 expression (Malin et al., 2011). Results from unbiased single-cell RNA-sequencing of mouse DRG obtained from cervical to lumbar levels reveal no specific coexpression of $K_V6.4$ in nociceptive Trpv1/Scn10a expressing neurones (Zeisel et al., 2018). However, single-cell RNA-sequencing of colonic sensory neurones identified that $K_V6.4$ does co-localise with Trpv1 and $Na_V1.8$ (Hockley et al., 2019), consistent with our findings here that $K_V6.4$, Trpv1 and $Na_V1.8$ are coexpressed in uterine sensory neurones from T12-L2 and L5-S2 DRG. Taken together, these data suggest that $K_V6.4$ might be a marker for sensory neurones that innervate the viscera. Due to the restricted expression of *Kcng4* in a particular sensory neurone type, expression of $K_V6.4$-Met419 is expected to reduce excitability specifically for this class of sensory neurones.

For the rare allele rs140124801 to modulate labour pain it needs to cause a significant change in $K_V6.4$-influenced neuronal activity, and to do so in the heterozygote state. Our electrophysiology and cell trafficking studies showed that the mutant $K_V6.4$-Met419, as opposed to $K_V6.4$, had no effect on $K_V2.1$ function, nor was it trafficked to the plasma membrane. Transfection of $K_V6.4$ into mouse sensory neurones produced a more hyperpolarised voltage-dependence of inactivation for the predicted heterotetrameric K_V2/silent K_V channel component of I_K than when $K_V6.4$-Met419 was transfected, further supporting the hypothesis that the loss-of-function $K_V6.4$-Met419 results in more $K_V2.1$ activity at positive voltages. $K_V2.1$ is known to contribute to the after-hyperpolarisation duration, intra-action potential refractory period, and thus regulate neuronal excitability (Tsantoulas et al., 2014). Hence, we anticipated that a $K_V6.4$-Met419-induced deficit in $K_V2.1$ function would likely result in fewer action potentials and thus less pain during periods of sustained nociceptor activity, such as that occurring with uterine contractions during labour. Although we did not observe a difference in the after-hyperpolarisation duration or action potential frequency between sensory neurones transfected with $K_V6.4$ or $K_V6.4$-Met419 (possibly due to the continual current injection used), we did find that a larger amount of current was required to cause $K_V6.4$-Met419 expressing neurones to fire actions potentials and thus conclude that the mutation confers reduced neuronal excitability (Figure 6). Critically, we observed that $K_V6.4$-Met419 has a dominant negative effect on $K_V6.4$, regarding modulation of the voltage-dependence of inactivation for $K_V2.1$. This result likely explains the reduction in labour pain seen in individuals in our cohort who were heterozygotes for the SNP rs140124801 rare allele. Although results contained herein demonstrate the effect of $K_V6.4$-Met419 on neuronal excitability, a further way to demonstrate this would be to generate either transgenic mice or use adeno-associated viruses to transduce sensory neurons innervating a specific target, as has recently been conducted with the knee (Chakrabarti et al.). Using mice overexpressing $K_V6.4$-Met419, we would hypothesise that like humans expressing the SNP rs140124801 rare allele, these $K_V6.4$-Met419 mice might have a raised threshold to acute noxious stimuli compared to wild type mice, as well as potentially having a reduced chronic pain phenotype, results that would align with the known roles of K_V channels in mouse pain

behaviour, for example, knockout of $K_V9.1$ leads to increased basal mechanical pain and exacerbates neuropathic pain (Tsantoulas et al., 2018).

Moreover, the importance of K_Vs in regulating neuronal excitability is highlighted by study of induced pluripotent stem cell derived sensory neurones (iPSC-SN) derived from a mother and son with inherited erythromelalgia (IEM) (Mis et al., 2019). Both individuals carry the same $Na_V1.7$ variant that is associated with IEM, but the frequency and duration of pain attacks differed, thus implicating further genetic variants. Whole exome sequencing of both individuals identified a *KCNQ2* variant, which encodes $K_V7.2$, in the individual experiencing less pain. Interestingly, the "less pain" variant resulted in a hyperpolarising shift in the $V_{1/2}$ for activation of the $K_V7.2$ mediated M current (a major determinant of RMP) and a more hyperpolarised RMP making it more difficult for APs to be evoked in iPSC-SNs. Thus, this study, alongside ours, demonstrates the importance of K_V function in modulating neuronal excitability and pain experience.

There is a growing understanding of the distinctions between the neural pathways for pain from visceral and somatic tissues: each have evolved nociceptors that sense damage in different physical environments (Bertucci and Arendt, 2013). Our findings suggest a key role for $K_V6.4$ in specifically regulating nociceptor excitability, and hence pain, in normal labour. $K_V6.4$ is also expressed in other parts of the nervous system (Figure S6C) and its expression in non-neural tissues is unknown. However, we found that women carrying the rare allele *KCNG4* managed nulliparous labour without analgesics, have higher experimental pain thresholds but are otherwise healthy without any psychological or cognitive abnormalities. Their phenotype suggests that the loss of modulatory effects of $K_V6.4$ is non- pathogenic in other parts of the nervous system and non-neural tissues. If druggable, $K_V6.4$ would be a potential target for modulating labour pain without the maternal and neonatal side effects inherent in other analgesic interventions in this setting. Our data also raise the question of whether $K_V6.4$ has roles in other painful visceral disorders, both within and outside the female genital tract. One closely related context would be primary dysmenorrhea, which is characterised by severe pain associated with uterine contraction during menstruation (Ju et al., 2014). Further development of selective $K_V6.4$ pharmacological agents is required to fully probe the role of $K_V6.4$ in visceral pain.

ACKNOWLEDGMENTS

The authors would like to thank the mothers who participated in this study. We acknowledge the support from the National Institute of Health Research who facilitated identification of potential participants. We thank midwives and other clinicians who assisted with case ascertainment and invited potential participants on our behalf. We would like to acknowledge Ingrid Scholtes and staff at the Cambridge NIHR Clinical Investigation Ward who cared for our participants during their visit.

Funding: MCL, DKM, DW, and CGW acknowledge funding from Addenbrooke's Charitable Trust and the NIHR Cambridge Biomedical Research Centre. MN was funded by the Wellcome Trust (200183/Z/15/Z); JH and ESS by a Rosetrees Postdoctoral Grant (A1296) and the BBSRC (BB/R006210/1); GC and ESS by Versus Arthritis Grants (RG21973); VBL and FR by the Wellcome Trust (106262/Z/14/Z and 106263/Z/14/Z) and a joint MRC programme within the Metabolic Diseases Unit (MRC_MC_UU_12012/3). EF, GI and CB were funded by the Cambridge NIHR Biomedical Research Centre Integrative Genomics theme and LAP by a BBSRC-funded studentship (BB/M011194/1). We thank Professor Naomichi Matsumoto and Professor Hirotomo Saitsu for the kind use of their KCNG4 vector. We would like to thank Walid Khaled for the kind loan of the Nucleofector key to electrophysiological experiments.

AUTHOR CONTRIBUTIONS

MCL, MSN, FR, DW, DKM, ESS and CGW made substantial contributions to the conception and design of this work. MCL, GI, CB and CGW made substantial contributions to the acquisition of clinical data. MSN, JRFH, VBL, LAP, GC and PE made substantial contributions to the acquisition of cell and molecular biology data. MCL, MSN, JRFH, VBL, LAP, ID, GC, KS, FR, EVF, PE, ESS and CGW made substantial contributions to the analysis and interpretation of data for the work. All authors were responsible for the drafting of the work or revising and giving final approval of the version to be published.

DECLARATION OF INTERESTS

None

MAIN FIGURES TITLES AND LEGENDS

Figure 1 Molecular genetics of *KCNG4* SNP rs140124801, and analysis of $K_V2.1$ inactivation properties (A) Summary of the genetic analysis. The resultant finding is of the SNP rs140124801 in *KCNG4*. Inset: electrophoretograms showing the alleles. (B) The nucleotide sequence of the SNP rs140124801 (NM_1.NM_172347.2) showing the altered GTG codon (in bold), and the rare allele (in red). Amino acids 416 to 423 of $K_V6.4$ (NP_758857.1) are shown below their nucleotide codons. The selectivity filter is in bold, and the wild type Val-419 shown above Met-419. (C) Evolutionary conservation of human $K_V6.4$ positions 408 to 426: rs140124801 alleles, representative proteins of each human K_V class, and of $K_V6.4$ in vertebrates. Invariant amino acids are capitalized. The selectivity filter TVGYG in yellow, and conserved aliphatic region in grey. Representative current recordings to determine $K_V2.1$ (D), $K_V2.1/K_V6.4$ (E), $K_V2.1/K_V6.4$-Met419 (F) steady-state inactivation properties. The applied voltage protocol is illustrated above (D). Vertical scale bar is 10 nA, horizontal scale bar is 0.5 s. Green traces indicate currents recorded during the −40 mV conditioning step. (G) Voltage-dependence of steady-state inactivation of $K_V2.1$ (grey filled circles, n = 9), $K_V2.1/K_V6.4$ (white squares, n = 12), and $K_V2.1/K_V6.4$-Met419 (black squares, n = 15). Symbols represent mean values, error bars indicate SEM. Solid lines represent the Boltzmann fitted curves.

Figure 2 p.Val419Met blocks $K_V6.4$ from reaching the plasma membrane independent of changes in steady-state expression (A) Immunofluorescence analysis of $K_V6.4$ localization. In the absence of $K_V2.1$, $K_V6.4$ was retained in the cytoplasm (white channel, top panel), and was trafficked to the cell membrane in the presence of $K_V2.1$ (white channel, 2nd panel down). In contrast, HA-tagged $K_V6.4$-Met419 did not localize to the cell membrane in either the absence or presence of $K_V2.1$ expression (white channels in the 3rd and 4th panel down). Expression of $K_V2.1$ is demonstrated by presence or absence of green nuclei, expression of $K_V6.4$ is displayed directly by HA tag in the white channel and expression of the IRES vector expressing $K_V6.4$ is displayed by presence of mCherry signal in the red channel. Graphs adjacent to each panel display the intensity of $K_V6.4$ HA signal along the red line in each respective white channel; note membrane localized peaks only in $K_V6.4$ when co-expressed with $K_V2.1$. Scale bars indicate 10 μm (B) HA-tagged $K_V6.4$ was transiently expressed in the presence or absence of $K_V2.1$. There was a modest reduction in steady state stability for $K_V6.4$-Met419 compared with $K_V6.4$. (C) Stability assessed by densitometry of HA compared with mCherry as a control of transfection efficiency, error bars indicate standard error. Unpaired t-test (P = 0.04).

Figure 3 *Kcng4* is coexpressed with *Kcnb1* in mouse uterine sensory neurones and expression of $K_V6.4$-Met419 in mouse sensory neurones increases the threshold for action potential discharge, compared to $K_V6.4$ (A) Uterine sensory neurones were retrogradely labelled using fast blue and harvested following dissociation. Scale bar 40μm. (B) Co-expression analysis of thoracolumbar (T12-L2, n = 44 cells) and lumbosacral (L5-S2, n = 45 cells) uterine sensory neurones expressing transcripts for *Kcng4*, *Kcnb1*, *Trpv1* and *Scn10a*. Each segment in the wheel-diagram is representative of a single cell, with a coloured segment signifying positive expression. (C) Representative current recordings to determine the voltage dependence of steady-state inactivation of the stromatoxin-1 (ScTx)-sensitive I_K elicited by the inset voltage protocol in the absence (C) and presence (D) of 100nM ScTx. Green traces indicate currents recorded during the −40 mV conditioning step. (E) The ScTx-sensitive I_K was obtained by subtraction of D from C. (F) Inactivation curves for the ScTx-sensitive I_K for neurones transfected with either $K_V6.4$ (n = 8) or $K_V6.4$-Met419 (n = 7). Both datasets were fit with a sum of two Boltzmann functions. The midpoints of both the 2nd components of these fits are plotted as either light dashed ($K_V6.4$) or heavy dashed ($K_V6.4$-Met419) lines. Each point and error bars indicate mean ± SEM. (G) Representative current clamp recordings of neurones of comparable capacitance transfected with either $K_V6.4$ or $K_V6.4$-Met419 showing action potentials evoked by ramp injection of current (0-1 nA, 1s). The thresholds for action potential discharge are annotated with light dashed ($K_V6.4$) or heavy dashed ($K_V6.4$-Met419) lines. Summary data of action potential thresholds obtained from neurones transfected with either $K_V6.4$ or $K_V6.4$-Met419 and untransfected controls obtained via a (H) ramp protocol (0-1 nA, 1s) or (I) step protocol (+10 pA, 50 ms). Red points represent cells that responded to 1 μM capsaicin in voltage clamp mode. Both recordings in Panel G were from cells which were capsaicin responders. Bars indicate mean values, error bars indicate SEM, n = 6-10, * $P < 0.05$, one-way ANOVA with Bonferroni's correction for multiple tests.

Figure 4 Sub-cellular localization and electrophysiology analysis of the dominant-negative effect of human $K_V6.4$-Met419 (A) HEK293 and HeLa cells (separate experiments) were transfected with $K_V2.1$ and either wild-type $K_V6.4$, $K_V6.4$-Met419 or equimolar concentrations of $K_V6.4/K_V6.4$-Met419. Cell membranes were stained with Na^+/K^+ ATPase (red channel) and HA-tagged $K_V6.4$ (green channel). HA-tagged $K_V6.4$ localized to the cell membrane, showing significant co-localization with Na^+/K^+ ATPase. Both $K_V6.4$-Met419 and $K_V6.4/K_V6.4$-Met419 co-expression showed cytoplasmic retention of $K_V6.4$ and no evidence of co-localization with Na^+/K^+ ATPase. Graphs below each pane display the profile of signal for membrane and $K_V6.4$.HA along the plane of the white line in the merged image. Note red and green signal co-localise in the $K_V6.4$ experiment and are distinct in the $K_V6.4$-Met419 and heterozygote experiment. Scale bars indicate 20 μm (B) Quantification of Pearson's co-localization co-efficient between $K_V6.4$.HA and Na^+/K^+ ATPase in each experimental condition. For each condition at least 17 cells were counted from three independent experiments. (C) Voltage of half-maximal inactivation from inactivation protocols shown in Figure 1D-

G. Co-expression of both $K_V6.4$ and $K_V6.4$-Met419 with $K_V2.1$ failed to evoke a shift in the voltage-dependence of inactivation. Bars indicate mean values, error bars indicate SEM, n = 9-15, *** $P < 0.001$. Statistics in B and C represent one-way ANOVA with Bonferroni's multiple comparisons test.

Figure 5 Effects of $K_V6.4$-Met419 on $K_V2.1$ heterotetramerisation. (A) Wild Type $K_V6.4$ co-immunoprecipitates with $K_V2.1$ when co-expressed in HEK293 cells (pulling down with $K_V2.1$ or HA-tagged $K_V6.4$). $K_V6.4$-Met419 disrupts binding to $K_V2.1$, and there is significantly reduced binding of HA-tagged $K_V6.4$ to $K_V2.1$ when co-expressed with untagged $K_V6.4$-Met419. B $K_V6.4$ traffics to the plasma membrane less efficiently when co-expressed with untagged $K_V6.4$-Met419, indicating a dominant negative effect. (C) Quantification of $K_V6.4$ membrane localization by Pearson's coefficient assessing colocalisation of HA and Na^+/K^+ ATPase membrane marker, data from three independent experiments. Error bars indicate SEM.

Figure 6 Schematic of the mechanism by which the rare allele SNP rs140124801 p.Val419Met in *KCNG4* (encoding voltage-gated potassium channel subunit $K_V6.4$) regulates neuronal excitability. (A) In most individuals, visceral nociceptors capable of transducing labour pain possess a combination of homomeric $K_V2.1$ channels and heteromeric $K_V2.1/K_V6.4$ channels, whereas in individuals with the rare allele SNP rs140124801 p.Val419Met in *KCNG4* (B) $K_V2.1/K_V6.4$-Met419 heteromers fail to traffic from the cytoplasm to the plasma membrane resulting in a greater proportion of $K_V2.1$ homomeric channels. Due to their steady-state inactivation properties, $K_V2.1/K_V6.4$ heteromers have reduced availability at more depolarised membrane potentials compared to $K_V2.1$ homomers and thus in nociceptors expressing $K_V6.4$-Met419 there is greater $K_V2.1$ homomer-mediated current at depolarized membrane potentials, which reduces neuronal excitability.

MAIN TABLES AND LEGENDS

Characteristics (at delivery of first-born)	Test cohort			Control cohort			P unadjusted	P adjusted *	CI5	CI95
	n	mean	SD	n	mean	SD				
Age (years)	39	32.83	4.18	33	31.94	3.98	0.33		-2.73	0.93
Head circumference of newborn (cm)	#26	34.00	0.98	+24	34.46	0.97	0.10		-0.10	1.01
Weight of newborn (g)	38	3362	434.1	33	3384	419.2	0.83		-180.90	224.76
Characteristics (at research visit)	**Test cohort**			**Control cohort**			P unadjusted	P adjusted *	CI5	CI95
	n	mean	SD	n	mean	SD				
Age (years)	39	36.26	4.18	33	36.45	4.11	0.62		-1.48	2.46
Upper arm diameter at assessment (cm)	39	28.54	3.60	33	29.23	3.63	0.43		-1.03	2.41
Sensory and pain thresholds										
Cold detection (°C)	39	30.45	0.93	33	30.35	0.95	0.79		-0.42	0.25
Warm detection (°C)	39	34.43	0.99	33	34.97	0.87	0.002	0.012	0.28	1.05
Cuff pressure detection (mmHg)	39	28.44	7.79	33	27.10	8.38	0.51		-5.00	1.33
Cold pain (°C)	39	11.64	8.26	33	16.88	9.03	0.02	0.114	1.17	9.73
Heat pain (°C)	39	44.08	2.85	33	42.36	3.40	0.018	0.103	-2.92	-0.27
Cuff pressure pain (mmHg)	39	166.7	54.74	33	113.03	42.96	0.00002	0.00012	-77.03	-30.13
Pain tolerance (cold immersion)										
Pre-immersion hand temperature (°C)	34	30.46	1.95	33	30.82	1.66	0.42		-0.53	1.24
Post-immersion hand temperature (°C)	##33	17.92	4.72	33	20.51	3.54	0.02	0.12	0.40	4.60
Latency to hand withdrawal (s)	##36	77.03	71.82	33	44.11	55.73	0.03	0.14	-38.0	-0.0000
Peak pain occurrence (0-100mm)	##35	80.19	27.39	33	79.04	28.99	0.71		-5.50	4.00
Peak pain intensity (0-100mm)	##35	54.29	17.26	33	65.82	13.20	0.004	0.02	3.20	18.1
SFMPQ (sensory)	36	8.47	3.82	33	10.97	4.00	0.010	0.049	0.62	4.38
SFMPQ (affective)	36	1.00	1.53	33	1.24	1.35	0.26		-0.00002	0.99995

Table 1 Key characteristics of test cohort comprising women who did not request or require analgesics during nulliparous term spontaneous labour and controls who did. n, number of participants; SD, standard deviation; * Sidak's correction; CI5-CI95, 5-95% confidence interval; # missing clinical record; ## equipment failure or unavailable; SFMPQ, short-form McGill's Pain Questionnaire

STAR METHODS

Resource availability

Lead contact

Further information and requests for resources and reagents should be directed to and will be fulfilled by the Lead Contact, Ewan St John Smith (mailto:es336@cam.ac.uk).

Material availability

Plasmid constructs generated in this study will be made available upon request, subject to ethical restrictions and Material Transfer Agreements.

Data and code availability

Clinical datasets supporting Table 1, S2 & S3 and Fig. S2 are available upon request, subject to ethical restrictions.

Fully anonymized SNP data supporting the exome analyses (Fig. 1A) are provided in a supplemental file 'Table S3 SNP allele frequency data.xlsx'

Experimental model and subject details

Human case ascertainment and recruitment

Labour pain is a complex experience and difficult to quantify (Bergh et al., 2015). Epidurals and inhalational analgesia are currently the most effective forms of pain relief in labour (Jones et al., 2012). Hence the rate of epidural use is a recognized surrogate measure for pain in clinical trials that assess the effectiveness of other forms of analgesia in labour (Levett et al., 2016). The use of inhalational analgesia is far commoner, particularly in nulliparous parturients where labour is considered more painful. A UK survey suggests that Entonox® use in labour at 80% and first-time mothers were more likely to use labour analgesia . Hence, the phenotype for less painful labour was defined operationally as nulliparous parturients who did not request nor use epidural, inhalational or opioid-based analgesia. This behavioural definition would have captured individuals with *SCN9A* channelopathy who reported entirely painless labour (Haestier et al., 2012).

The studies commenced in October 2012 after National Research Ethics Service and Human Research Authority approval (Reference: 12-EE-0369) was granted. For the first study (Study A), potential participants were identified based at maternity units in the United Kingdom and invited via post to contact the research team. The post included an information sheet stating that the study sought "to use genetic analysis to look for variations in genes in women who do not feel as much pain as might be expected during childbirth, and determine whether such variation in pain experience might be related to genetic differences' and the invitation was for women that 'have had a baby and according to our records, you required minimal or no pain relief during the birth of your first child".

All potential participants who contacted the research team were further screened via telephone interview for eligibility (Table S1). Eligible participants were posted study information and a saliva sampling kit (Oragene®-DNA, OG-500, Genotek), with a self-addressed return envelope. Participants did not receive any financial incentive for the genetic study.

In the second study (Study B), women who had consented to the genetic study and for whom exome sequencing was successful were invited to the Cambridge NIHR Clinical Investigation Ward for further study. Those who were eligible (Table S1) and consented to participate comprised the test cohort.

Women who met the study criteria but who required analgesia during labour served as case controls. Controls were informed via participant information leaflet we have *"identified women who did not use painkillers during the birth of their first child. However, we are still unsure whether they are actually less sensitive to pain. In order to find out, we need to test their pain sensitivity and compare their results to women who did used an Epidural or Entonox (gas and air) for pain relief during their first labour"*. Controls were selected to match age at delivery of first-born, location of maternity unit and age at study visit. A total of 1029 invitations were sent by post. Where available, data on birth weight of baby and head circumference were recorded. The age range for the test and control cohorts were 27 to 48 years, and 28 to 44 years respectively (Table 1).

Participants were reimbursed up to maximum of 25GDP for time in addition to travel expenses for the two-hour visit. All participants and the researchers who communicated directly with them remained blind to genotype during the study.

Cell lines and culture conditions

HEK293 and HeLa cells were cultured in 90 % Dulbecco's modified Eagle medium (DMEM) supplemented with 10 % fetal bovine serum (FBS), 100 U/ml penicillin-streptomycin (pen-strep), and 2 mM L-glutamine at 37 °C, 5 % CO_2, 100 % humidity. Transfections were carried out using FugeneHD transfection reagent (Promega) according to the manufacturer's protocols. For co-expression studies, cloned $K_V2.1$ and $K_V6.4$ constructs were transfected at a ratio of 1:2. Cells for experiments were plated out on glass coverslips for immunostaining or 35 mm plastic dishes for electrophysiological recordings, 1-2 days prior to the experiment.

Animals

Adult C57BL/6J mice (Envigo), male and female, aged between 8 to 12 weeks, were conventionally housed in groups of 4-5 with nesting material and a red plastic shelter and various enrichment toys; the holding room was temperature controlled (21 °C) and mice were on a 12-hour/light dark cycle with food and water available *ad libitum.* Work was regulated under the Animals (Scientific Procedures) Act 1986 Amendment Regulations 2012 following ethical review by the University of Cambridge Animal Welfare and Ethical Review Body.

Method details

Clinical questionnaires, cognitive and sensory testing

A single research assistant in the same temperature-controlled room conducted all assessments. Participants were seated for the assessment and rest breaks were provided between assessments to minimize fatigue. Instructions for each assessment were read from a written script. These assessments were completed in the following sequence: (1) questionnaires administered on paper Hospital Anxiety and Depression Scale (HADS) (Zigmond and Snaith, 1983), Pain Catastrophizing Scale (PCS) (Sullivan et al., 1995), Multidimensional Health Locus of Control Scale (MHLC) (Stevens et al., 2011) and Life Orientation Test-Revised (LOTR) (Scheier et al., 1994), (2) quantitative sensory testing (QST) to determine stimulus detection, pain and tolerance thresholds, and (3) computerized cognitive assessments implemented on CANTAB® (Cambridge Cognition, UK) (Robbins et al., 1998). Hospital Anxiety and Depression Scale (HADS) (Zigmond and Snaith, 1983), Pain Catastrophizing Scale (PCS) (Sullivan et al., 1995), Multidimensional Health Locus of Control Scale (MHLC) (Stevens et al., 2011) and Life Orientation Test-Revised (LOTR) (Scheier et al., 1994).

Cambridge Neuropsychological Test Automated Battery (CANTAB)

The cognitive assessments were drawn from the Cambridge Neuropsychological Test Automated Battery (CANTAB) (http://www.cambridgecognition.com/). The computerised tests required finger-tap responses via touchscreen and are largely independent of verbal instruction. CANTAB software was deployed on an XGA-touch panel 12-inch monitor (Paceblade Slim-book P120; PaceBlade Technology). The sequence of tasks employed in the study was as follows: Motor Screening Task (MOT), Spatial Working Memory (SWM), Rapid Visual Information Processing (RVIP), Intra- Extra-Dimensional Set Shift (IED) and One-Touch Stockings of Cambridge (OTS). Descriptions of each task are provided below. All tasks were performed using the index finger of the dominant hand.

Motor Screening Task (MOT)

Coloured crosses are presented in different locations on the screen, one at a time. The participant must select the cross on the screen as quickly and accurately as possible. Outcome measures are (a) mean latency and (b) mean error, which reflect accuracy.

Spatial Working Memory (SWM)

The task assesses ability to retain spatial information and manipulate items in working memory. It is considered a sensitive measure of frontal lobe and executive dysfunction. This is a self-ordered task which also assesses heuristic strategy. Several coloured squares (box) are displayed in random locations on the touch screen. There is pre-set number of boxes with a blue token. The participant taps on a box to uncover a blue 'token' and place that token into a ‘bin’. The participant must remember which box has been tapped or emptied. The number of boxes is gradually increased until the participants is searching for tokens in a

total of eight boxes. The colour and position of boxes used are changed from trial to trial to discourage use of stereotyped search strategies. Outcome measures are (a) strategy, for which the fully efficient strategy would result in no boxes being revisited. A high score represents poor use of this strategy and a low score equates to effective use, and (b) total errors, which is the number of times a box is selected that cannot contain a blue token and therefore should not have been visited by the subject.

Rapid Visual Information Processing (RVP)

A white box is shown in the centre of the screen, inside which digits from 2 to 9 appear in a pseudo-random order, at the rate of 100 digits per minute. Participants are asked to detect target sequences of digits (for example, 2-4-6, 3-5-7, 4-6-8) and respond by tapping on a button-box as quickly as possible. Outcome measures are (a) sensitivity index A', which reflects how good the subject is at detecting target sequences, regardless of error tendency A score close to +1.00 indicates that a high true positive rate, and (b) response criterion B', which reflects the tendency to respond regardless of whether the target sequence is present. A score close to +1.00 indicates a high true negative rate.

Intra-Extra Dimensional Set

This task assesses visual discrimination and attentional set formation maintenance, shifting and flexibility of attention. IED task requires participants to learn the rule and select the correct icon (a specific shape or line). The task builds in complexity as distractors are added and the rule changes. The rule changes are both intra-dimensional (e.g. shapes are still the relevant set, but a different shape is now correct) and extra-dimensional (e.g. shapes are no longer the relevant set, instead one of the line stimuli is now correct). Outcome measures are (a) total errors (adjusted), which is a measure of the participant's efficiency. Whilst she may pass all nine stages, a substantial number of errors may be made in doing so. The errors are adjusted to account for those who fail at any stage of the test and hence have had less opportunity to make errors, (b) number of stages completed, and (c) total trials (adjusted), which is the number of trials completed on all attempted stages for each stage not attempted due to failure at an earlier stage.

One Touch Stockings of Cambridge

This task is a test of executive function, based upon the Tower of Hanoi. The participant is shown two displays containing three coloured balls. The displays are presented in such a way that they can be easily perceived as stacks of coloured balls held in stockings suspended from a beam. The participant is shown how to move the balls in the lower display to copy the pattern in the upper display and completes one demonstration problem, where the solution requires one move. The participant must then complete three further problems, one each requiring two moves, three moves and four moves. Next the participant is shown further problems and must work out mentally the number of moves the solutions require and then select the appropriate box at the bottom of the screen to indicate their response. Outcome measures are (a) mean choice to correct, which is the mean number of attempts to the correct response, and (b) mean latency to correct, which is the overall latency (time required) to the correct response.

Quantitative sensory testing

Stimulus detection and pain thresholds for heat and cold were determined by applying a 3x3 cm^2 thermode on the volar surface of the non-dominant mid-forearm (TSA, Medoc, Israel). The procedure was adapted from a clinical research protocol(Rolke et al., 2006b), for which the research assistant received formal training (Universitsmedizin Mannheim). Stimulus detection and pain thresholds were determined using increasing or decreasing temperature ramp of $1°C.s^{-1}$ from a baseline temperature of 32°C, with low and high safety cut-offs at 0 and 50°C respectively. Participants were instructed to click on a button when they first experience the required sensations. Four trials each with an inter-trial interval of 10s were employed to assess heat and cold stimulus detection thresholds. Three trials with a longer inter-trial interval of 30s were employed for heat and cold pain thresholds to minimize risks of burn.

Pressure detection and pain threshold were determined by cuff algometry(Vargas et al., 2006) applied to the dominant upper arm. The circumference of the upper arm was measured to determine the appropriate sphygmomanometer cuff size. A digital metronome (Korg MA-1, UK) was used to guide manual inflation of the cuff at 10 mmHg every 5s. The participant was instructed to verbally report when the point the cuff was felt to be 'just gripping' and when the gripping became just about painful, at which point the cuff pressure was rapidly released. The pressures at thresholds were recorded. The participant was then asked to indicate when all evoked sensation in the arm had resolved. The entire procedure was repeated thrice.

Pain tolerance was measured as latency to withdrawal from immersion of hand in a cold water bath (3 °C) (Mitchell et al., 2004). The participant was instructed to immerse her non-dominant hand and wrist into a circulating cold-water bath (RW2025G, Medline Scientific UK) and to withdraw the hand *ad libitum* when pain became intolerable. The maximum duration of cold-water immersion allowed was 180s, after which the participant was told to remove her hand from the water bath. All participants were told that there was a maximum allowable duration for immersion for safety but not the exact duration to avoid anticipatory effects.

The skin temperature of the hand dorsum was measured (NC 150, Microlife, Switerland) within 60s pre-immersion and 10s post-immersion (after the hand was wiped dry). Participants were then asked to rate peak intensity of pain during immersion using a 100mm visual analogue scale (VAS) with the left and right anchors labelled as 'no pain' and 'worst imaginable pain' respectively. They were also asked to estimate when the intensity of pain peaked during the period of immersion (100mm VAS; 0mm and 100mm represented the times of hand immersion and hand withdrawal respectively). Finally, participants completed the Short-Form McGill Pain Questionnaire (SQ-MPQ). The questionnaire comprises 15 pain descriptors: 11 pertain to sensory-discriminatory aspects (e.g. 'hot-burning'), and the rest pertained to affective-motivational (e.g. 'cruel-punishing') of the pain experienced during cold-water immersion of the hand (Melzack, 1987).

Genetic analysis of non-synonymous functional single nucleotide polymorphism alleles

For the genetic analysis of the discovery cohort we used the fSNPd approach (Stouffer et al., 2017). In brief, the hypothesis is that some individuals with a defined phenotype (in our case reduced labour pain inferred by the absence of analgesia requirement during labour) could have genetic predisposition(s) that explain their difference in phenotype. To be detected, such a genetic predisposition would have to be dominantly inherited and often penetrant: this is the case with many known autosomal dominant Mendelian genetic disorders such as Tuberose Sclerosis and Neurofibromatosis type 1 where the phenotype is variable (and can be incomplete) despite an individual carrying the known pathogenic familial mutation. The fSNPd approach further hypothesizes that the phenotype will not be caused by very rare genetic mutations, but by the rare alleles of known SNPs where the allele difference is protein changing. Examples of such SNPs exist that only cause a human phenotype when the heterozygous individual is exposed to a specific environmental insult or trigger, e.g. aminoglycoside induced deafness (Prezant et al., 1993) and SNPs rs267606617 and rs267606618; and carbamazepine associated toxic epidermal necrolysis and rs3909184 (Chung et al., 2004).

An exome analysis was performed on the genomic DNA of the 100 individuals of the discovery cohort by Beijing Genomics Institute using the Agilent 51M kit sequenced to an average of 50-fold coverage, as previously described (Nahorski et al., 2018). Such an analysis does not include all coding exons of all human genes, and for this reason SNPs in some genes are not assessed, and other SNPs were not assessed in all individuals in the discovery cohort (Stouffer et al., 2017). The exome vcf, bam and bam.bai files were iteratively analysed extracting data on all SNP in or near to exons, including the depth and quality of the sequence data, and the alleles detected (Stouffer et al., 2017). For each SNP the allele frequencies were compared to normal values, and deviations assessed for significance using a Chi-squared test with two tails and Yates correction. The resulting *P* values were subject separately to a Bonferroni correction and false discovery rate (FDR) correction, as approximately 100,000 SNPs were assessed in our fSNPd method. We then filtered only for clear-cut protein changing SNPs (mis-sense mutations predicted deleterious by SIFT, nonsense mutations, splice site mutations, start codon mutations, and within-exon deletions and duplications), as such changes are potentially more amenable to function tests of pathogenicity; reducing from 18,106 SNPs prior to SIFT and pathogenicity analysis to 3,596 afterwards. We then further filtered only for SNPs within ion channel genes, as members of this group of genes have already been implicated in Mendelian pain disorders, and testing techniques for ion channel function are well established; resulting in 28 SNPs (Stevens and Stephens, 2018). For all SNPs, especially those whose rare allele frequency is < 5 %, geographical and ethnic differences must be considered; rs140124801 has a rare allele frequency in EVS of 0.0051 (cohort size 6500), in gNOMAD Europeans = 0.0072 (cohort size 18,878), 1000 Genome = 0.0048 (cohort size 2,504), and our population were Caucasian and predominantly born in the United Kingdom.

In the discovery cohort we assessed all individual bam files with the Integrated Genome Viewer to determine which rs140124801 alleles were present, blind of the fSNPd results. All individuals predicted to have the

rs140124801 rare allele were Sanger sequenced and complete concordance was found. Primers were designed with Primer3 and are available on request. Genomic DNA of the 58 individuals in the replication cohort was Sanger sequenced to determine the SNP rs140124801 allele frequencies. The allele frequency and number of heterozygotes of rs140124801 was assessed in combined cohort of discovery and replication by Chi^2 test with two tailed and Yates correction (for small numbers), using the more conservative control population allele frequency of 0.0072 for heterozygote carriers.

We assessed the effects on protein sequence and protein function of the *KCNG4* SNP rs140124801 alleles by use of bioinformatic resources within the Human Genome Browser, NCBI BLASTP for protein sequence comparisons and Conserved Domains (CD search) for detecting if the amino acid change occurred within a known protein domain and SIFT for pathogenicity prediction.

Modelling of *KCNG4* alleles on the $K_V2.1/K_V6.4$ heterotetramer

We used the X-ray crystallography derived structure of rat $K_V2.1$ homotetramer (RCSB Protein Data Bank ID: 3LNM) to model the effects of the rare allele of rs140124801 (Tao et al., 2010). Rat and human subunits form both $K_V2.1$ homotetramers and 3:1 $K_V2.1$:$K_V6.4$ heterotetramers. Rat was the closest species to humans with a published $K_V2.1$ protein structure. Rat and human $K_V2.1$ proteins are 94% identical and 79% identical for $K_V6.4$. However, restricting the alignment to the 78 amino-acid region physically adjacent to the K^+ selectivity filter (the pore loop from transmembrane region 5 to transmembrane region 6, which includes the K^+ selectivity filter) rat and human $K_V2.1$, they are identical and rat and human $K_V6.4$ is 96% identical (with no amino acid changes in the aliphatic pocket or selectivity filter).

We used structure 3LNM and the Cn3D software (Wang et al., 2000) to examine the K^+ selectivity filter of the $K_V2.1$ homotetramer to look at the sites of interaction of each of the four individual $K_V2.1$ proteins, and produced images where proteins and individual amino acids were identifiable, or could be omitted from the whole tetrameric structure.

The K^+ ion selectivity filter is formed by the peptide backbone carbonyl groups of the amino acids TVGYG of each of the four K_V subunits. This forms a narrow central channel through which potassium ions (K^+) can flow out of the cell. Each K_V subunit forms an identical quarter of the tetramer structure about the selectivity filter region central pore. The $K_V2.1$ homotetramer model reveals the side chains of the Valine and Tyrosine of each subunit selectivity filter TVGYG protruding into a highly conserved "aliphatic pocket" (with canonical sequence WWAIIS, see Figure 1C) in the adjacent K_V subunit. In this model the Valine-419 of $K_V6.4$ can be accommodated identically compared with the equivalent Valine-374 of $K_V2.1$. However, the larger aliphatic side chain of 419-Methionine in the $K_V6.4$ SNP would not be able to be accommodated within the aliphatic pocket, and hence would disrupt the ion selectivity region of the $K_V2.1/2.1/2.1/6.4$ heterotetramer.

DNA constructs and antibodies

A full-length human *KCNG4* cDNA clone was purchased from Source bioscience (IRCMp5012B0629D) and cloned in-house into a pcDNA3 based expression plasmid (CMV-genex-polioIRESmCherry) both with or without a C-terminal HA tag. The p.Val419Met mutation was introduced by site-directed mutagenesis (Stratagene) according to the manufacturer's protocols and sequences of the plasmids were confirmed by Sanger Sequencing. The clone expressing $K_V2.1$ alongside a nuclear GFP reporter in the pCAGGS-IRES2-nucEGFP vector has been described previously (Saitsu et al., 2015) and was a kind gift from Prof. Hiromoto Saitsu.

Antibodies used were anti-HA mouse monoclonal (12B12, #MMS-101P, Biolegend), anti-Na^+/K^+ ATPase rabbit monoclonal (ab76020, Abcam), anti-mCherry rat monoclonal (M11217), anti-β-actin mouse monoclonal (a2228, Sigma), anti-$K_V2.1$ rabbit polyclonal (APC-012, Alomone), anti-$K_V6.4$ mouse monoclonal (N458/10, NeuroMab), anti-$K_V2.1$ mouse monoclonal (K89/34, ab192761, Abcam), and anti-HA rabbit monoclonal (C29F4 #3724, Cell Signalling).

Immunofluorescence analysis and confocal microscopy

HEK293 and HeLa cells were cultured on poly-L-lysine coated coverslips and transfected as described above. 48-hours after transfection, cells were fixed by 10 minutes incubation in 4 % paraformaldehyde. Cells were permeabilized by 10 minutes incubation in 0.3 % Triton-X100 solution followed by 30 minutes at room temperature in 5 % BSA solution. Alternatively, when staining for Na^+/K^+ ATPase, cells were fixed and permeabilized by emersion in ice cold methanol. Fixed cells were then stained with primary antibodies for 1 hour in 5 % BSA and fluorescent secondary antibody also for 1 hour. Secondary antibodies used were Alexa Fluor 488 donkey anti-mouse, Alexa Fluor 546 goat anti-rabbit, Alexa Fluor 546 donkey anti-mouse, Alexa Fluor 633 goat anti-mouse (all from Life Technologies). Coverslips were mounted onto glass slides using Prolong Diamond Antifade Mountant with DAPI (Molecular Probes). Cells were visualised with an LSM880 confocal microscope.

Co-immunoprecipitation

HEK293 cells were transfected with $K_V2.1$ and $K_V6.4$ plasmid constructs as described in the associated figures, and harvested after 3 days. Co-immunoprecipitation was carried out using the Dynabeads Co-Immuniprecipitation Kit (Life Technologies) according to the manufacturers protocols. Antibodies used were anti-HA mouse monoclonal (12B12, #MMS-101P, Biolegend), anti-$K_V2.1$ rabbit polyclonal (APC-012, Alomone), anti $K_V2.1$ mouse monoclonal (K89/34, ab192761, Abcam), and anti-HA rabbit monoclonal (C29F4 #3724, Cell Signalling). IP buffer supplied in the kit was supplemented with 80mM NaCl.

Electrophysiological characterization of *KCNG4* SNP rs140124801 alleles and *KCNB1* in HEK293 cells

Whole-cell recordings from transfected HEK293 cells were performed using 1-2.5 MΩ resistance fire-polished borosilicate glass electrodes filled with an internal pipette solution containing (in mM): KCl (110), K_4-BAPTA (5), HEPES (10), $MgCl_2$ (1), K_2ATP (5), pH 7.3, 281 mOsm/kg. Cells were continuously superfused with bath solution containing (in mM): NaCl (145), KCl (4), HEPES (10), D-glucose (10), $CaCl_2$ (1.8) $MgCl_2$ (1), pH 7.4, 300 mOsm/kg, at room temperature (20-24 °C). Potassium currents (I_K) were recorded in voltage clamp mode using an Axopatch 200B connected through a Digidata 1440A A/D converter and pCLAMP software (version 10, Axon Instruments). The calculated linear leakage current was digitally subtracted offline for all current measurements. Potassium currents were elicited by step depolarisations from a holding potential of −90 mV to various test potentials. The voltage-dependence of activation was determined from tail currents recorded from a 200 ms voltage step to −60 mV following these various test potentials. The normalised tail currents were plotted against the voltage of the step depolarisations and fit with a Boltzmann function. A double pulse protocol was used to measure the voltage-dependence of steady-state inactivation. The protocol consisted of a 5 s prepulse that ranged between −110 to +40 mV from a holding potential of −90 mV followed by a 200 ms test pulse to +50 mV. Normalised currents during this test pulse were plotted against the prepulse voltage and fit with a Boltzmann function. The time course of recovery from inactivation was investigated by applying a 5 s prepulse to +20 mV from a holding potential of −90 mV and applying a 200 ms test pulse to +20 mV at various time intervals after the conditioning prepulse. Recoveries from inactivation time courses were fit to a single exponential function.

Single-cell qRT-PCR of mouse uterus innervating sensory neurons

Uterus innervating sensory neurons were retrograde labelled and the mRNA transcript expression for genes of interest determined using methodology previously described for other visceral organs (Hockley et al., 2019; Peiris et al., 2017; Prato et al., 2017). Female C57BL/6J mice (10-12 weeks) were used. Following laparotomy, 2 injections (~2.5 µl/injection) of Fast Blue (FB: 2% in saline) were made, one into each uterine horn adjacent to the cervix. Following recovery, animals were provided a soft, glucose-enriched diet and prophylactic post-operative analgesia (buprenorphine 0.05-0.1 mg kg^{-1}). After 5-8 days, mice were killed by cervical dislocation and two primary cultures made from DRG T12-L2 (TL) and L5-S2 (LS), respectively. Dissected DRG were incubated in Lebovitz L-15 Glutamax (Thermo Fisher Scientific, UK) media containing 6 mg ml^{-1} bovine serum albumin (BSA, Sigma-Aldrich) and 1 mg ml^{-1} collagenase type 1A (Sigma-Aldrich, UK) for 15 min at 37 ºC in 5 % CO_2. After a further 30 min incubation in L-15 media containing 1mg ml^{-1} trypsin (Sigma-Aldrich) and 6 mg ml^{-1} BSA, ganglia were triturated and dissociated cell-containing supernatant collected by repeat brief centrifugation (5 x 500 *g*). TL and LS neurons were plated on poly-D-lysine coated coverslips (BD Biosciences, UK) and incubated in L-15 growth media

(containing 2 % penicillin/streptomycin, 24 mM $NaHCO_3$, 38 mM glucose and 10 % fetal bovine serum). Fluorescently labelled FB-positive cells were picked manually by pulled glass pipette into 9 µl mastermix (containing 5 µl CellsDirect 2 x reaction buffer (Invitrogen, UK), 2.5 µl 0.2 x primer-probe mix against genes of interest, 0.1 µl SUPERase-in (Ambion, USA), 1.2 µl TE buffer (Applichem, Germany) and 0.2 µl Superscript III Reverse Transcriptase-Platinum Taq mix (Invitrogen, UK)), bath samples were collected as negative controls and all samples immediately frozen on dry ice. Prior to 1:5 dilution in TE buffer, reverse transcription and preamplification of cDNA was performed by thermal cycling (50 °C for 30 min, 95 °C for 2 min, then 24 cycles of 95 °C for 15 s, 60 °C for 4 min). Gene-specific Taqman qPCR assays were then run (Taqman Assay ID: *Kcng4*, Mm01240890_m1; *Kcnb1*, Mm00492791_m1; *Trpv1*, Mm01246300_m1; *Scn10a*, Mm00501467_m1; *Gapdh*, Mm99999915_g1; Applied Biosystems) with the following thermal cycling protocol (50 °C for 2 min, 95 °C for 10 min, then 40 cycles of 95 °C for 15 s, 60 °C for 1 min). The expression of glyceraldehyde-3-phosphate dehydrogenase (*Gapdh*) acted as an internal positive control and was present in all single-cell RT-PCR products and absent in bath control samples. 15 uterine sensory neurons per region (TL and LS) per mouse ($N = 3$) were collected. In total, 90 neurons were collected, and photos taken for analysis of cell diameter. qPCR products were detected in 89 neurons and quantitative assessment of gene expression was determined by quantification cycle values less than the threshold of 35 considered positive.

Whole-cell patch-clamp recordings

Primary DRG cultures from C57BL/6J mice (8-10 weeks) were generated using the methodology described for single-cell qRT-PCR experiments with the following exceptions. From each mouse, DRG T10-S1 were dissected and pooled into a single primary culture. After trituration, in order to purify the DRG culture to improve transfection efficiency, dissociated cells were subjected to a 3.5 % BSA (in L-15 media) density gradient centrifugation (20 mins at 20 *g*) and the supernatant discarded. The remaining purified dissociated neurons were washed once in L-15 growth media before resuspension in 100 µl of Mouse Neuron Nucleofector solution (Amaxa Mouse Neuron Nucleofector Kit, Lonza, UK) containing 4.5 µg plasmid of either wild-type K_V6.4 or K_V6.4-Met419 in a CMV-KCNG4-polioIRESmCherry expression cassette. Incorporation of the plasmid was achieved by electroporation (Program O-0005; Nucleofector IIb, Lonza, UK) and cells plated on poly-D-lysine/laminin coated coverslips (BD Biosciences, UK) and incubated at 37 °C in 5 % CO_2 and L-15 growth media. Electrophysiology experiments were conducted 48-hours post-transfection, neurons positive for mCherry fluorescence were selected following excitation with a 572 nm LED (Cairn Research, UK).

To assess voltage-gated K^+ currents, patch pipettes were pulled using a P-97 pipette puller (Sutter Instruments, USA) with typical resistances of 3-5 MΩ and back-filled with the pipette solution containing (in mM): KAspartate (110), KCl (30), $MgCl_2$ (2), $CaCl_2$ (1), Na_2ATP (5), EGTA (2), cAMP (0.1), HEPES (10), pH 7.4. Recordings were obtained using a Multiclamp 700A amplifier (Molecular Devices, USA) in the voltage-clamp mode and digitised using a Digidata 1440A (Molecular Devices). Voltage errors were

minimized using 70% series resistance compensation. Mouse neurons were continuously superfused with the bath solution containing (in mM): N-methyl-D-glucamine (NMDG; 140), KCl (5), $MgCl_2$ (1), $CaCl_2$ (1.8), glucose (10), HEPES (5), pH 7.4. The osmolality of both solutions was adjusted to 300-310 mOsm. Cells with series resistance values greater than 15 MΩ were omitted from analysis.

I_K activation and inactivation protocols (Figures 3 and S5) were applied after achieving whole-cell rupture. Using a rapid change perfusion system (Intracel EVH-9, UK), 100 nM Stromatoxin-1 (Alomone, Israel) in bath solution was applied to the cells for 3 minutes prior to repeating activation and inactivation protocols. Thus ScTx-sensitive I_K was determined by subtraction of the post-ScTx I_K from the pre-ScTx I_K in pClamp software (Molecular Devices). The voltage-dependence of I_K activation was fitted with the following Boltzmann equation: $y = t / (1 + \exp((V_{50} - E)/k))$, where E is the applied voltage, V_{50} is the voltage at which 50 % of the channels are activated, t is the top of the curve, and k is the slope factor. Whilst the voltage-dependence of I_K inactivation was fitted with the sum of two Boltzmann equations: $y = (tF / (1 + \exp((_1V_{50} - E) /_1k)) + (t(1 - F) / (1 + \exp((_2V_{50}-E)/_2k)$, where E is the applied voltage, $_1V_{50}$ is the voltage at which 50 % of the 1st component channels are inactivated, $_2V_{50}$ is the voltage at which 50 % of the 2nd component channels are inactivated, t is the top of the curve, $_1k$ is the slope factor for the first component and $_2k$ for the second component, and F defines the relative component contribution.

For current clamp experiments a HEKA EPC-10 amplifier (Lambrecht, Germany) and the corresponding Patchmaster software were used. The extracellular solution contained (in mM): NaCl (140), KCl (4), $MgCl_2$ (1), $CaCl_2$ (2), glucose (4) and HEPES (10), pH 7.40. Patch pipettes, pulled as for I_K experiments, were filled with intracellular solution containing (in mM): KCl (110), NaCl (10), $MgCl_2$ (1) EGTA (1), HEPES (10), Na_2ATP (2), Na_2GTP (0.5), pH 7.3. After gaining access to cells and entering current clamp mode the resting membrane potential of neurons was noted. Ramp depolarisation from 0 pA to 1 nA over a period of 1 s was first used to assess action potential threshold. A step protocol (Δ10 pA, 50 ms) was then used to confirm thresholds. The ability of neurons to fire multiple action potentials was assessed by applying a suprathreshold (2x the threshold determined by step protocol) for 500 ms. Lastly, capsaicin (1 μM in extracellular solution) sensitivity was assessed in voltage clamp mode; neurons that produced an inward current, time-locked to a 5 s application were considered responders. Only cells which fired action potentials and had a resting membrane potential less than or equal to -40 mV were taken through to analyses. Action potential parameters were measured from those evoked by the step protocol using Fitmaster software (HEKA) and IgorPro (Wavemetrics).

Quantification and statistical analyses

For psychometric and quantitative sensory testing, statistical analyses were performed with R Studio (Version 1.1.442). The mean and standard deviation were generated for each outcome variable for test and control cohorts. Shapiro-Wilk tests and F-tests were used assess data normality and differences in variances. Differences between the means of each outcome variable in test and control cohorts were assessed using

tests for two independent samples, using Student's *t*-test, Welch's *t*-test or Mann-Whitney U tests when the relevant assumptions were met. The level of statistical significance was adjusted using Sidak's correction. The correction applied to multiple outcomes associated with each domain of assessments: questionnaires, CANTAB, sensory detection, pain thresholds and tolerance.

For statistical assessment of the genetic data collected in this study, enrichment of amino acid altering SNPs was assessed by exome sequencing, with exome vcf, bam and bam.bai files iteratively analyzed to extract data on all SNPs in or near to exons, including the depth and quality of the sequence data, and the alleles detected (Stouffer et al., 2017). For each SNP the allele frequencies were compared to normal values derived from the 1000 genomes project and exome variant server, and deviations assessed for significance using a Chi-squared test with two tails and Yates correction. The resulting *P* values were subject separately to a Bonferroni and FDR correction, as approximately 100,000 SNPs were assessed in our fSNPd method.

We then focused only on ion channels, defined as being identified by the Gene Ontology Term GO:0005216 (423 genes, which were also hand curated and checked against a Pfizer/Neusentis database that had been shared with us). There were 28 SNPs found in ion channels and each was in a different gene; there was only one detected SNP in *KCNG4*. Eight of these SNPs were then eliminated because the protein change caused by the rare allele was common in the orthologous mammalian proteins. For the remaining 20 SNPs, we determined the allele frequency of each of the by use of the Integrated Genome Viewer examining the cohort's exome bam files individually. This led to the elimination of 19 SNPs, 14 as the common allele frequency was 100% and program errors in assigning alleles within our discovery cohort had falsely appeared to show a deviation from 100%, and five because of misalignment of reads to homologous genes leading to errors in SNP allele calling and SNP allele frequency calculation.

Further statistical tests used to assess differences between $K_V6.4$ and $K_V6.4$-Met419 in the cellular and animal studies are unpaired *t*-tests and ANOVA with Bonferroni's multiple comparison post-hoc test, as described in the relevant figure legends. Differences between groups were considered significant at a *P* value < 0.05, and were tested using GraphPad (Prism5.0, California, USA).

Key resources table

REAGENT or RESOURCE	SOURCE	IDENTIFIER
Antibodies		
Anti-HA mouse monoclonal	Biolegend	12B12, #MMS-101P
Anti-K_V2.1 rabbit polyclonal	Alomone	APC-012
Anit-K_V2.1 mouse monoclonal	Abcam	ab192761
Anti-HA rabbit monoclonal	Cell Signalling	C29F4 #3724
Anti-Na^+/K^+ ATPase rabbit monoclonal	Abcam	Ab76020
Anti β-actin mouse monoclonal	Sigma Aldrich	A2228
Anti-mCherry rat monoclonal	ThermoFisher	M11217
Bacterial and Virus Strains		
Biological Samples		
Chemicals, Peptides, and Recombinant Proteins		
Trypsin	Sigma-Aldrich	T4799
Collagenase	Sigma-Aldrich	C5138
Bovine serum albumin	Sigma-Aldrich	B2064
Fast Blue	Polysciences	17740
Trypsin from Bovine Pancreas	Sigma-Aldrich	T9935
Collagenase, Type 1A	Sigma-Aldrich	C9891
Capsaicin	Sigma-Aldrich	M2028
Stromatoxin-1	Alomone	STS-350
FuGENE HD transfection reagent	Promega	E2311
Critical Commercial Assays		
CellsDirect One-Step qRT-PCR kit	Invitrogen	11753100
Amaxa Mouse Neuron Nucleofactor kit	Lonza	VPG-1001
Dynabeads Co-Immuniprecipitation Kit	ThermoFisher	14321D
Kcng4 Taqman primer-probe	Applied Biosciences	Mm01240890_m1
Kcnb1 Taqman primer-probe	Applied Biosciences	Mm00492791_m1
Trpv1 Taqman primer-probe	Applied Biosciences	Mm01246300_m1
Scn10a Taqman primer-probe	Applied Biosciences	Mm00501467_m1
Gapdh Taqman primer-probe	Applied Biosciences	Mm99999915_g1
Deposited Data		
Experimental Models: Cell Lines		
HeLa	Sigma Aldrich	93021013
HEK293	Sigma Aldrich	85120602
Experimental Models: Organisms/Strains		
C57BL/6J mice	Envigo	Wild-type
Oligonucleotides		

Recombinant DNA		
KCNG4 cDNA clone in polioIRESmCherry w/wo HA tag	This manuscript	
$K_V2.1$ in pCAGGS-IRES2-nucEGFP	Gift from Prof Saitsu	Saitsu et al., 2015
KCNG4.Met419 cDNA clone in polioIRESmCherry w/wo HA tag	This manuscript	
Software and Algorithms		
R Studio Version 1.2.5036 for Mac	R	https://rstudio.com/products/rstudio/
pClamp (v10.3)	Molecular Devices	pClamp (v10.3)
Prism (v8)	GraphPad	Prism (v8)
Patchmaster	HEKA	heka.com
Fitmaster v2x90.4	HEKA	heka.com
Igor pro v6.37	WaveMetrics	wavemetrics.com
Patcher's Power Tools	Max-Planck-Institut	https://www3.mpibpc.mpg.de/groups/neher/index.php?page=aboutppt
Step One version 2.3	Applied Biosystems	N/A
Other		
Poly-D-lysine and laminin coated coverslips	BD Biosciences	354087
Nucleofector IIb	Lonza	AAB-1001
Multiclamp 700A amplifier	Molecular Devices	N/A
Digidata 1440A	Molecular Devices	N/A
Rapid change perfusion system	Intracel	EVH-9
EPC-10 amplifier	HEKA	N/A
Pipette puller	Sutter Instruments	P-97
Lebovitz L015 Glutamax	Thermo Fisher Scientific	31415029
Poly-D-lysine coated coverslips	BD Biosciences	354086
SUPERase-inhibitor	Ambion	AM2696

985

986

REFERENCES

The National Perinatal Epidemiology Unit: Safely delivered: a national survey of women's experience of maternity care 2014. https://www.npeu.ox.ac.uk/.

Bennett, D.L., Clark, A.J., Huang, J., Waxman, S.G., and Dib-Hajj, S.D. (2019). The Role of Voltage-Gated Sodium Channels in Pain Signaling. Physiol Rev 99, 1079-1151.

Bergh, I.H., Johansson, A., Bratt, A., Ekstrom, A., and Martensson, L.B. (2015). Assessment and documentation of women's labour pain: A cross-sectional study in Swedish delivery wards. Women Birth 28, e14-18.

Bertucci, P., and Arendt, D. (2013). Somatic and visceral nervous systems - an ancient duality. BMC Biol 11, 54.

Bocksteins, E. (2016). Kv5, Kv6, Kv8, and Kv9 subunits: No simple silent bystanders. J Gen Physiol 147, 105-125.

Bocksteins, E., Labro, A.J., Snyders, D.J., and Mohapatra, D.P. (2012). The electrically silent Kv6.4 subunit confers hyperpolarized gating charge movement in Kv2.1/Kv6.4 heterotetrameric channels. PLoS One 7, e37143.

Bocksteins, E., Raes, A.L., Van de Vijver, G., Bruyns, T., Van Bogaert, P.P., and Snyders, D.J. (2009). Kv2.1 and silent Kv subunits underlie the delayed rectifier K+ current in cultured small mouse DRG neurons. American journal of physiology Cell physiology 296, C1271-1278.

Bocksteins, E., and Snyders, D.J. (2012). Electrically silent Kv subunits: their molecular and functional characteristics. Physiology (Bethesda) 27, 73-84.

Bocksteins, E., Snyders, D.J., and Holmgren, M. (2017). Independent movement of the voltage sensors in KV2.1/KV6.4 heterotetramers. Sci Rep 7, 41646.

Carvalho, B., Zheng, M., and Aiono-Le Tagaloa, L. (2013). Evaluation of experimental pain tests to predict labour pain and epidural analgesic consumption. Br J Anaesth 110, 600-606.

Carvalho, B., Zheng, M., and Aiono-Le Tagaloa, L. (2014). A prospective observational study evaluating the ability of prelabor psychological tests to predict labor pain, epidural analgesic consumption, and maternal satisfaction. Anesth Analg 119, 632-640.

Chakrabarti, S., Pattison, L.A., Doleschall, B., Rickman, R.H., Blake, H., Callejo, G., Heppenstall, P.A., and Smith, E.S.J. Intra-articular AAV-PHP.S mediated chemogenetic targeting of knee-innervating dorsal root ganglion neurons alleviates inflammatory pain in mice. Arthritis & Rheumatology n/a.

Chung, W.H., Hung, S.I., Hong, H.S., Hsih, M.S., Yang, L.C., Ho, H.C., Wu, J.Y., and Chen, Y.T. (2004). Medical genetics: a marker for Stevens-Johnson syndrome. Nature 428, 486.

Cuello, L.G., Jogini, V., Cortes, D.M., and Perozo, E. (2010). Structural mechanism of C-type inactivation in K(+) channels. Nature 466, 203-208.

Escoubas, P., Diochot, S., Celerier, M.L., Nakajima, T., and Lazdunski, M. (2002). Novel tarantula toxins for subtypes of voltage-dependent potassium channels in the Kv2 and Kv4 subfamilies. Mol Pharmacol 62, 48-57.

Gruss, L.T., and Schmitt, D. (2015). The evolution of the human pelvis: changing adaptations to bipedalism, obstetrics and thermoregulation. Philos Trans R Soc Lond B Biol Sci 370, 20140063.

Haestier, A., Hamilton, S., and Chilvers, R.J. (2012). Labour outcomes in siblings with channelopathy associated insensitivity to pain due to bi-alleleic SCN9A mutations. Obstetric Medicine 5, 181-182.

Herweijer, G., Kyloh, M., Beckett, E.A., Dodds, K.N., and Spencer, N.J. (2014). Characterization of primary afferent spinal innervation of mouse uterus. Front Neurosci 8, 202.

Hockley, J.R.F., Taylor, T.S., Callejo, G., Wilbrey, A.L., Gutteridge, A., Bach, K., Winchester, W.J., Bulmer, D.C., McMurray, G., and Smith, E.S.J. (2019). Single-cell RNAseq reveals seven classes of colonic sensory neuron. Gut 68, 633-644.

Jones, L., Othman, M., Dowswell, T., Alfirevic, Z., Gates, S., Newburn, M., Jordan, S., Lavender, T., and Neilson, J.P. (2012). Pain management for women in labour: an overview of systematic reviews. Cochrane Database Syst Rev, CD009234.

Ju, H., Jones, M., and Mishra, G. (2014). The prevalence and risk factors of dysmenorrhea. Epidemiol Rev 36, 104-113.

Labor, S., and Maguire, S. (2008). The Pain of Labour. Rev Pain 2, 15-19.

Levett, K.M., Smith, C.A., Bensoussan, A., and Dahlen, H.G. (2016). Complementary therapies for labour and birth study: a randomised controlled trial of antenatal integrative medicine for pain management in labour. BMJ open 6, e010691.

Loeser, J.D., and Treede, R.D. (2008). The Kyoto protocol of IASP Basic Pain Terminology. Pain 137, 473-477.

Malin, S., Molliver, D., Christianson, J.A., Schwartz, E.S., Cornuet, P., Albers, K.M., and Davis, B.M. (2011). TRPV1 and TRPA1 function and modulation are target tissue dependent. J Neurosci 31, 10516-10528.

Maul, A. (2007). An evolutionary interpretation of the significance of physical pain experienced by human females: defloration and childbirth pains. Med Hypotheses 69, 403-409.

Melzack, R. (1984). The myth of painless childbirth (the John J. Bonica lecture). Pain 19, 321-337.

Melzack, R. (1987). The short-form McGill Pain Questionnaire. Pain 30, 191-197.

Melzack, R., and Schaffelberg, D. (1987). Low-back pain during labor. Am J Obstet Gynecol 156, 901-905.

Mis, M.A., Yang, Y., Tanaka, B.S., Gomis-Perez, C., Liu, S., Dib-Hajj, F., Adi, T., Garcia-Milian, R., Schulman, B.R., Dib-Hajj, S.D., and Waxman, S.G. (2019). Resilience to Pain: A Peripheral Component Identified Using Induced Pluripotent Stem Cells and Dynamic Clamp. J Neurosci 39, 382-392.

Mitchell, L.A., MacDonald, R.A., and Brodie, E.E. (2004). Temperature and the cold pressor test. J Pain 5, 233-237.

Nahorski, M.S., Maddirevula, S., Ishimura, R., Alsahli, S., Brady, A.F., Begemann, A., Mizushima, T., Guzman-Vega, F.J., Obata, M., Ichimura, Y.*, et al.* (2018). Biallelic UFM1 and UFC1 mutations expand the essential role of ufmylation in brain development. Brain 141, 1934-1945.

Ottschytsch, N., Raes, A.L., Timmermans, J.P., and Snyders, D.J. (2005). Domain analysis of Kv6.3, an electrically silent channel. J Physiol 568, 737-747.

Peiris, M., Hockley, J.R., Reed, D.E., Smith, E.S.J., Bulmer, D.C., and Blackshaw, L.A. (2017). Peripheral KV7 channels regulate visceral sensory function in mouse and human colon. Mol Pain 13, 1744806917709371.

Prato, V., Taberner, F.J., Hockley, J.R.F., Callejo, G., Arcourt, A., Tazir, B., Hammer, L., Schad, P., Heppenstall, P.A., Smith, E.S., and Lechner, S.G. (2017). Functional and Molecular Characterization of Mechanoinsensitive "Silent" Nociceptors. Cell Rep 21, 3102-3115.

Prezant, T.R., Agapian, J.V., Bohlman, M.C., Bu, X., Oztas, S., Qiu, W.Q., Arnos, K.S., Cortopassi, G.A., Jaber, L., Rotter, J.I., and et al. (1993). Mitochondrial ribosomal RNA mutation associated with both antibiotic-induced and non-syndromic deafness. Nat Genet 4, 289-294.

Robbins, T.W., James, M., Owen, A.M., Sahakian, B.J., Lawrence, A.D., McInnes, L., and Rabbitt, P.M. (1998). A study of performance on tests from the CANTAB battery sensitive to frontal lobe dysfunction in a large sample of normal volunteers: implications for theories of executive functioning and cognitive aging. Cambridge Neuropsychological Test Automated Battery. J Int Neuropsychol Soc 4, 474-490.

Rolke, R., Baron, R., Maier, C., Tolle, T.R., Treede, R.D., Beyer, A., Binder, A., Birbaumer, N., Birklein, F., Botefur, I.C.*, et al.* (2006a). Quantitative sensory testing in the German Research Network on Neuropathic Pain (DFNS): standardized protocol and reference values. Pain 123, 231-243.

Rolke, R., Magerl, W., Campbell, K.A., Schalber, C., Caspari, S., Birklein, F., and Treede, R.D. (2006b). Quantitative sensory testing: a comprehensive protocol for clinical trials. Eur J Pain 10, 77-88.

Saitsu, H., Akita, T., Tohyama, J., Goldberg-Stern, H., Kobayashi, Y., Cohen, R., Kato, M., Ohba, C., Miyatake, S., Tsurusaki, Y.*, et al.* (2015). De novo KCNB1 mutations in infantile epilepsy inhibit repetitive neuronal firing. Sci Rep 5, 15199.

Scheier, M.F., Carver, C.S., and Bridges, M.W. (1994). Distinguishing optimism from neuroticism (and trait anxiety, self-mastery, and self-esteem): a reevaluation of the Life Orientation Test. J Pers Soc Psychol 67, 1063-1078.

Sherwood, C.C., Bauernfeind, A.L., Bianchi, S., Raghanti, M.A., and Hof, P.R. (2012). Human brain evolution writ large and small. Prog Brain Res 195, 237-254.

Stevens, E.B., and Stephens, G.J. (2018). Recent advances in targeting ion channels to treat chronic pain. Br J Pharmacol 175, 2133-2137.

Stevens, N.R., Hamilton, N.A., and Wallston, K.A. (2011). Validation of the multidimensional health locus of control scales for labor and delivery. Research in nursing & health 34, 282-296.

Stouffer, K., Nahorski, M., Moreno, P., Sarveswaran, N., Menon, D., Lee, M., and Geoffrey Woods, C. (2017). Functional SNP allele discovery (fSNPd): an approach to find highly penetrant, environmental-triggered genotypes underlying complex human phenotypes. BMC Genomics 18, 944.

Sullivan, M.J.L., Bishop, S.R., and Pivik, J. (1995). The Pain Catastrophizing Scale: Development and validation. Psychological Assessment 7, 524-532.

Tao, X., Lee, A., Limapichat, W., Dougherty, D.A., and MacKinnon, R. (2010). A gating charge transfer center in voltage sensors. Science 328, 67-73.

Tsantoulas, C., Denk, F., Signore, M., Nassar, M.A., Futai, K., and McMahon, S.B. (2018). Mice lacking Kcns1 in peripheral neurons show increased basal and neuropathic pain sensitivity. Pain 159, 1641-1651.

Tsantoulas, C., Zhu, L., Yip, P., Grist, J., Michael, G.J., and McMahon, S.B. (2014). Kv2 dysfunction after peripheral axotomy enhances sensory neuron responsiveness to sustained input. Exp Neurol 251, 115-126.

Vargas, A., Vargas, A., Hernandez-Paz, R., Sanchez-Huerta, J.M., Romero-Ramirez, R., Amezcua-Guerra, L., Kooh, M., Nava, A., Pineda, C., Rodriguez-Leal, G., and Martinez-Lavin, M. (2006). Sphygmomanometry-evoked allodynia--a simple bedside test indicative of fibromyalgia: a multicenter developmental study. Journal of clinical rheumatology : practical reports on rheumatic & musculoskeletal diseases 12, 272-274.

Wang, Y., Geer, L.Y., Chappey, C., Kans, J.A., and Bryant, S.H. (2000). Cn3D: sequence and structure views for Entrez. Trends Biochem Sci 25, 300-302.

Wheeler, D.W., Lee, M.C.H., Harrison, E.K., Menon, D.K., and Woods, C.G. (2014). Case Report: Neuropathic pain in a patient with congenital insensitivity to pain. F1000Research 3, 135.

Whitburn, L.Y., Jones, L.E., Davey, M.A., and Small, R. (2017). The meaning of labour pain: how the social environment and other contextual factors shape women's experiences. BMC Pregnancy Childbirth 17, 157.

Zeisel, A., Hochgerner, H., Lonnerberg, P., Johnsson, A., Memic, F., van der Zwan, J., Haring, M., Braun, E., Borm, L.E., La Manno, G.*, et al.* (2018). Molecular Architecture of the Mouse Nervous System. Cell 174, 999-1014 e1022.

Zhong, X.Z., Abd-Elrahman, K.S., Liao, C.H., El-Yazbi, A.F., Walsh, E.J., Walsh, M.P., and Cole, W.C. (2010). Stromatoxin-sensitive, heteromultimeric Kv2.1/Kv9.3 channels contribute to myogenic control of cerebral arterial diameter. J Physiol 588, 4519-4537.

Zigmond, A.S., and Snaith, R.P. (1983). The hospital anxiety and depression scale. Acta Psychiatr Scand 67, 361-370.

Figure 1

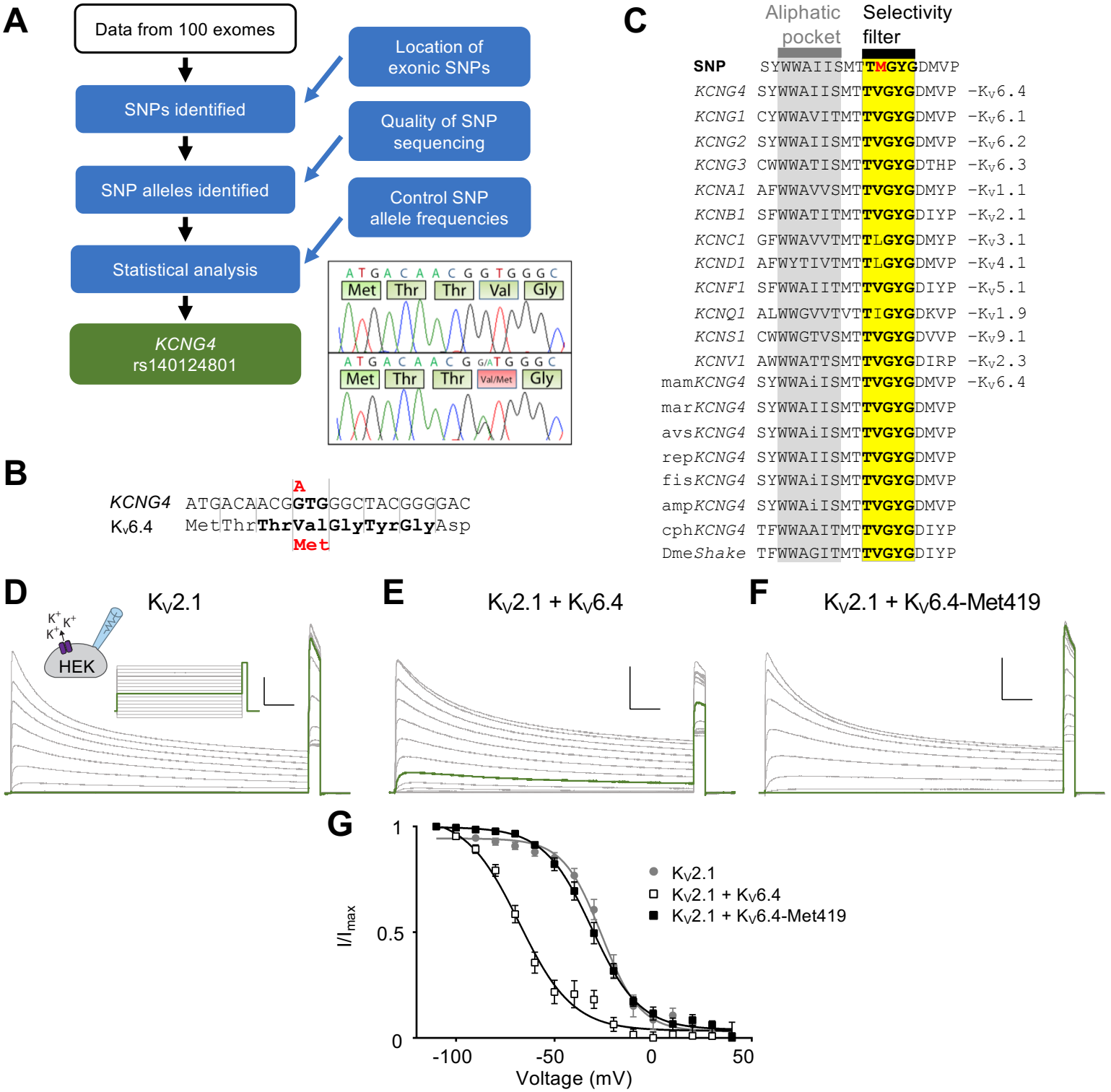
A
Data from 100 exomes
SNPs identified
SNP alleles identified
Statistical analysis
KCNG4
rs140124801
Location of exonic SNPs
Quality of SNP sequencing
Control SNP allele frequencies
ATGACAACGGTGGGC
Met Thr Thr Val Gly
ATGACAACGG/ATGGGC
Met Thr Thr Val/Met Gly
B
KCNG4 ATGACAACGGTGGGCTACGGGGAC
Kv6.4 MetThrThrValGlyTyrGlyAsp
A
Met
C
Aliphatic pocket
Selectivity filter
SNP SYWWAIISMTTMGYGDMVP
KCNG4 SYWWAIISMTTVGYGDMVP -Kv6.4
KCNG1 CYWWAVITMTTVGYGDMVP -Kv6.1
KCNG2 SYWWAIISMTTVGYGDMVP -Kv6.2
KCNG3 CWWWATISMTTVGYGDTHP -Kv6.3
KCNA1 AFWWAVVSMTTVGYGDMYP -Kv1.1
KCNB1 SFWWATITMTTVGYGDIYP -Kv2.1
KCNC1 GFWWAVVTMTTLGYGDMYP -Kv3.1
KCND1 AFWYTIVTMTTLGYGDMVP -Kv4.1
KCNF1 SFWWAIITMTTVGYGDIYP -Kv5.1
KCNQ1 ALWWGVVTVTTIGYGDKVP -Kv1.9
KCNS1 CWWWGTVSMTTVGYGDVVP -Kv9.1
KCNV1 AWWWATTSMTTVGYGDIRP -Kv2.3
mamKCNG4 SYWWAiISMTTVGYGDMVP -Kv6.4
marKCNG4 SYWWAIISMTTVGYGDMVP
avsKCNG4 SYWWAiISMTTVGYGDMVP
repKCNG4 SYWWAIISMTTVGYGDMVP
fisKCNG4 SYWWAiISMTTVGYGDMVP
ampKCNG4 SYWWAiISMTTVGYGDMVP
cphKCNG4 TFWWAAITMTTVGYGDIYP
DmeShake TFWWAGITMTTVGYGDIYP
D
Kv2.1
K+ K+ K+
HEK
E
Kv2.1 + Kv6.4
F
Kv2.1 + Kv6.4-Met419
G
I/Imax
1
0.5
0
-100
-50
0
50
Voltage (mV)
Kv2.1
Kv2.1 + Kv6.4
Kv2.1 + Kv6.4-Met419

Figure 2

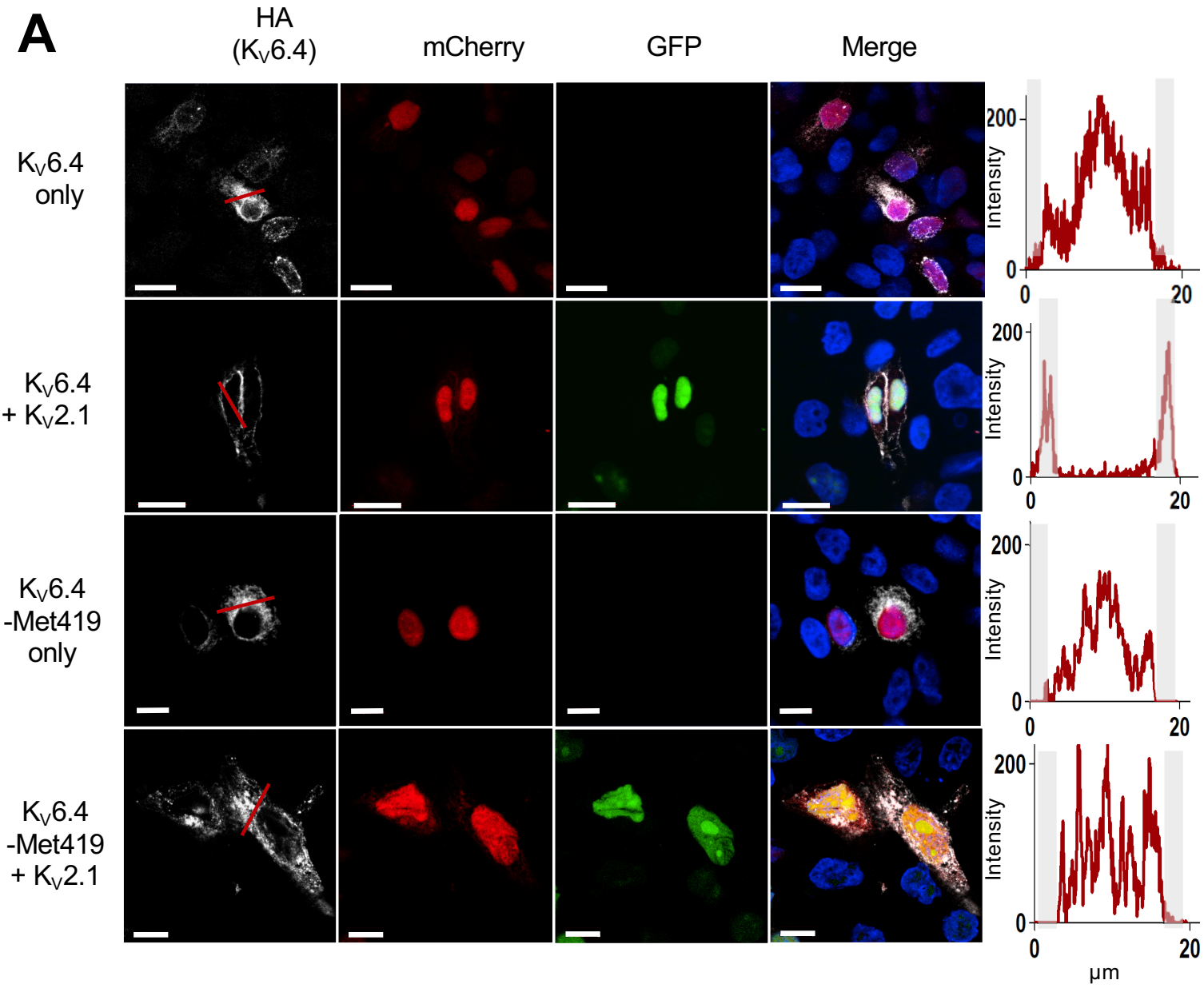
A
HA
(KV6.4)
mCherry
GFP
Merge
KV6.4
only
KV6.4
+ KV2.1
KV6.4
-Met419
only
KV6.4
-Met419
+ KV2.1
Intensity
200
0
20
μm

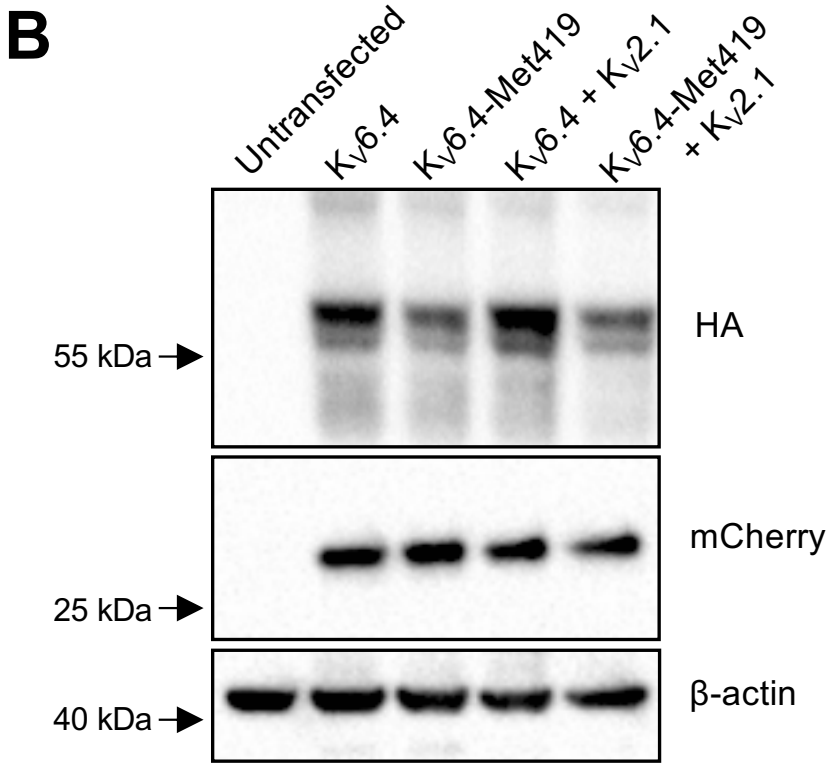
B
Untransfected
KV6.4
KV6.4-Met419
KV6.4 + KV2.1
KV6.4-Met419
+ KV2.1
55 kDa
25 kDa
40 kDa
HA
mCherry
β-actin

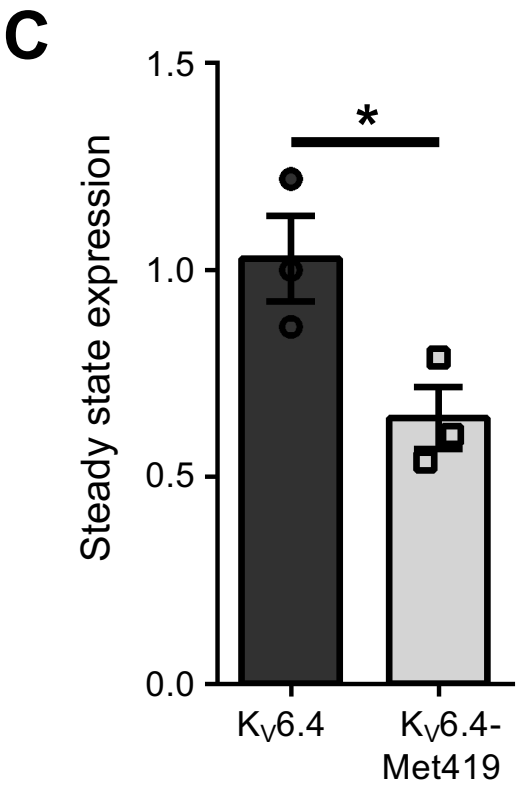
C
Steady state expression
1.5
1.0
0.5
0.0
*
KV6.4
KV6.4-
Met419

Figure 3

Click here to access/download;Figure;Fig 3.tiff

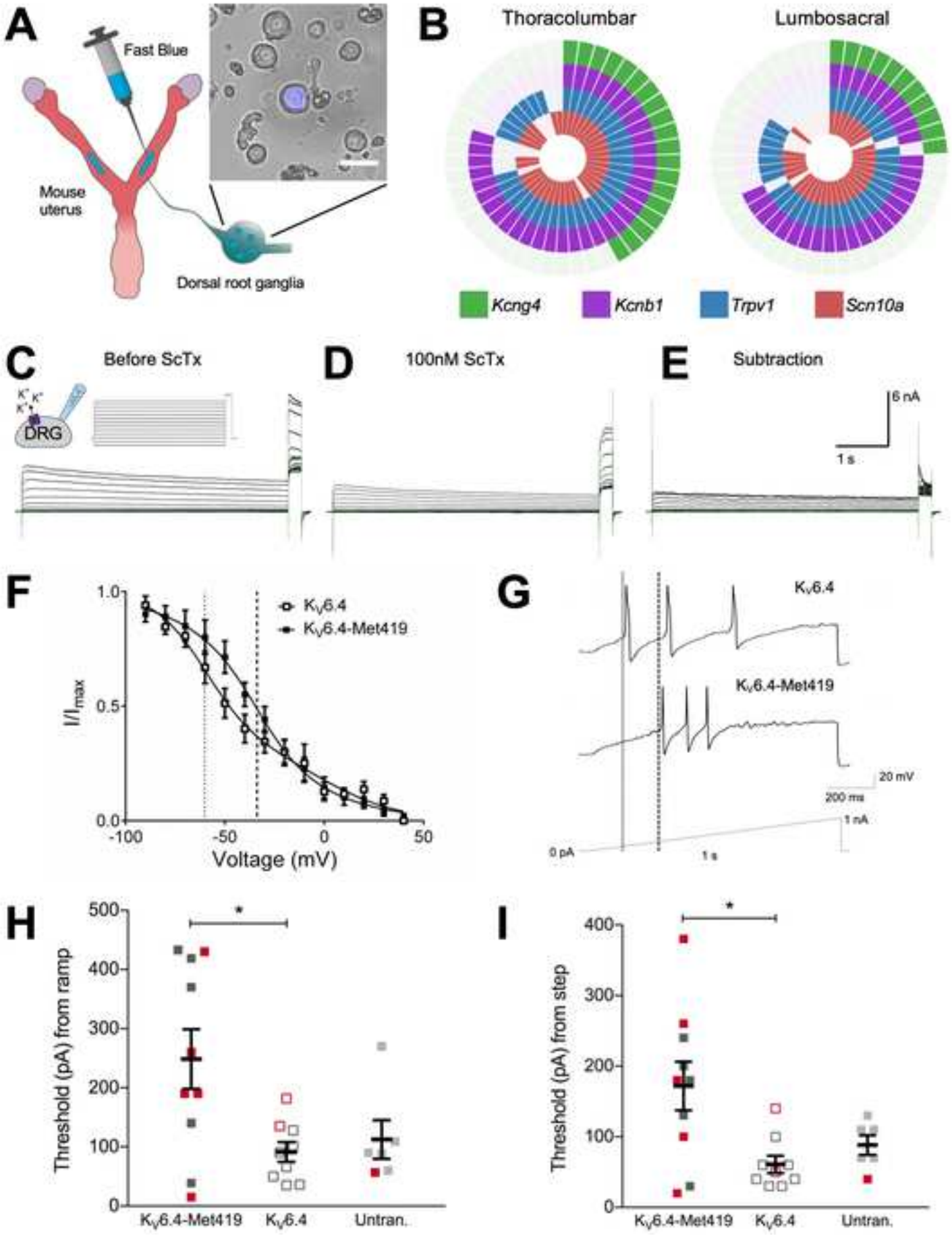

Figure 4

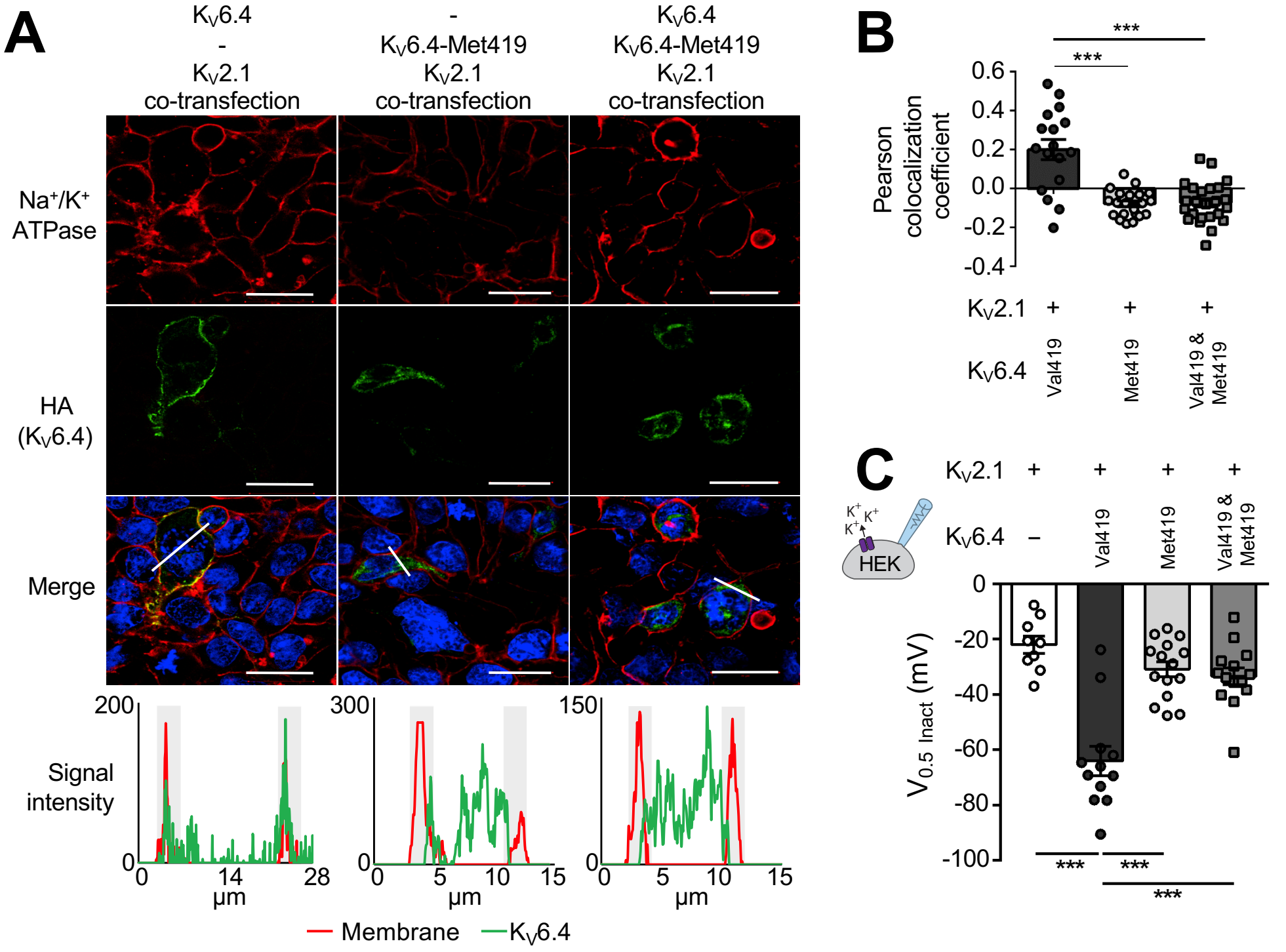
A
K_V6.4
-
K_V2.1
co-transfection
-
K_V6.4-Met419
K_V2.1
co-transfection
K_V6.4
K_V6.4-Met419
K_V2.1
co-transfection
Na^+/K^+ ATPase
HA (K_V6.4)
Merge
Signal intensity
200
0
0
14
28
µm
300
0
0
5
10
15
µm
150
0
0
5
10
15
µm
Membrane
K_V6.4
B
***
***
Pearson colocalization coefficient
0.6
0.4
0.2
0.0
-0.2
-0.4
K_V2.1 + + +
K_V6.4 Val419 Met419 Val419 & Met419
C
HEK
K^+ K^+ K^+
K_V2.1 + + + +
K_V6.4 – Val419 Met419 Val419 & Met419
$V_{0.5\ Inact}$ (mV)
0
-20
-40
-60
-80
-100
***
***
***

Figure 5

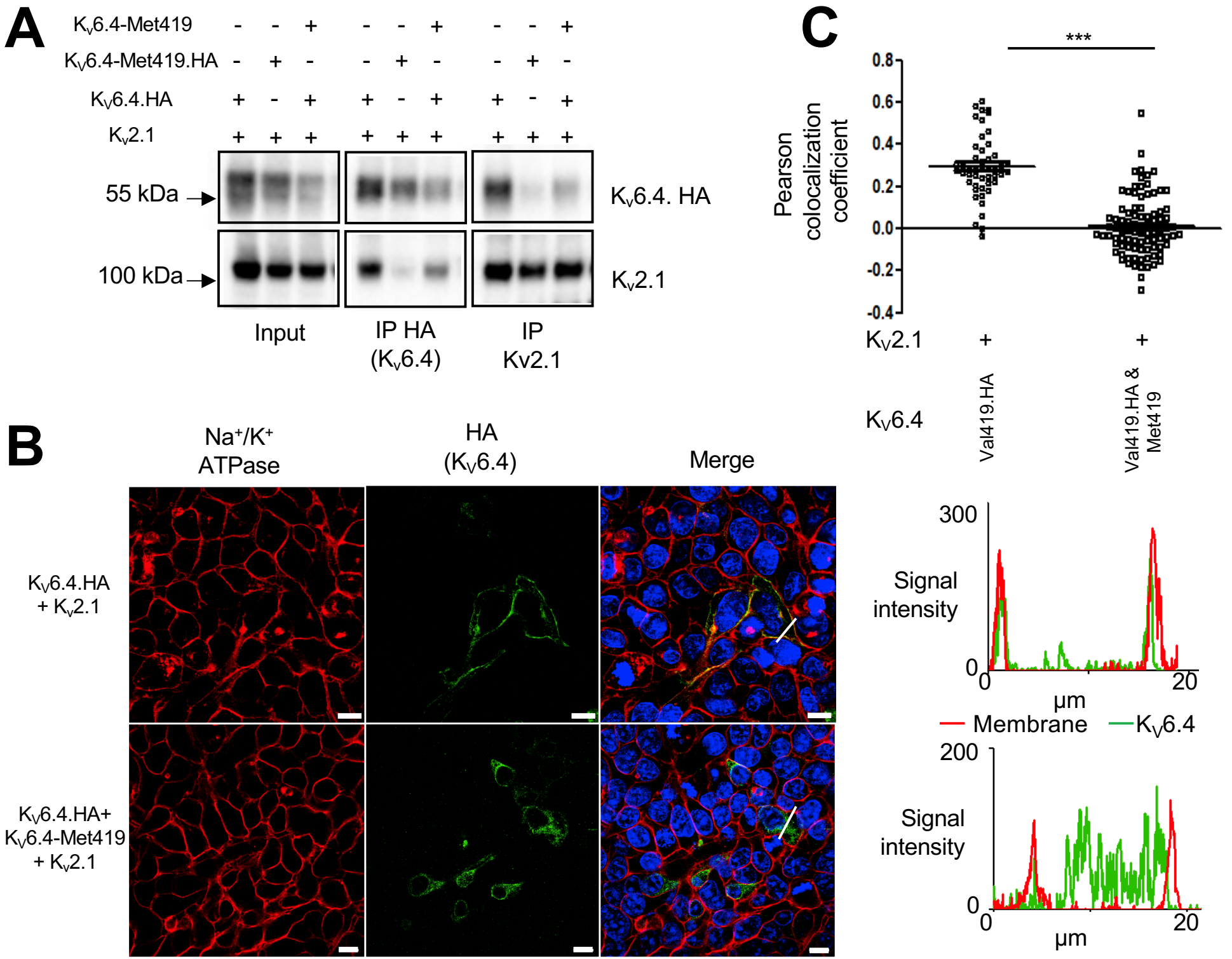
A
Kv6.4-Met419
Kv6.4-Met419.HA
Kv6.4.HA
Kv2.1
55 kDa
100 kDa
Kv6.4. HA
Kv2.1
Input
IP HA (Kv6.4)
IP Kv2.1
C
***
Pearson colocalization coefficient
0.8
0.6
0.4
0.2
0.0
-0.2
-0.4
Kv2.1 + +
Kv6.4 Val419.HA Val419.HA & Met419
B
Na+/K+ ATPase
HA (Kv6.4)
Merge
Kv6.4.HA + Kv2.1
Kv6.4.HA+ Kv6.4-Met419 + Kv2.1
300
Signal intensity
0
0
20
µm
Membrane
Kv6.4
200
Signal intensity
0
0
20
µm

Figure 6

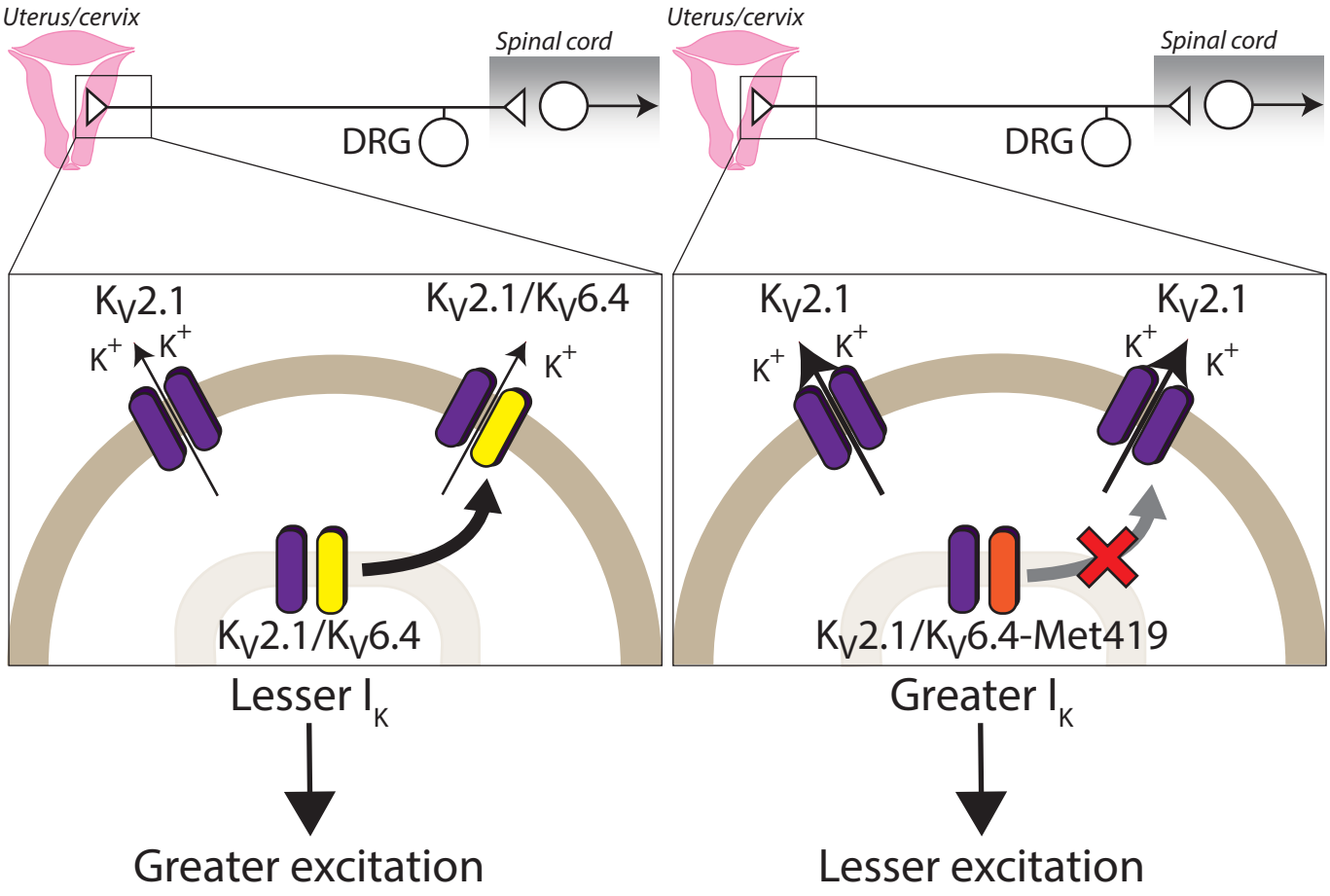
Uterus/cervix
Spinal cord
DRG
$K_V2.1$
$K_V2.1/K_V6.4$
K^+
$K_V2.1/K_V6.4$
Lesser I_K
Greater excitation
Uterus/cervix
Spinal cord
DRG
$K_V2.1$
$K_V2.1$
K^+
$K_V2.1/K_V6.4$-Met419
Greater I_K
Lesser excitation

Study A DNA Sampling

Inclusion Criteria

Females who are

- Aged 18 years and above
- Able to communicate in English
- Caucasian
- Able to provide written and informed consent
- Who experienced term (beyond 37 week gestation) spontaneous vaginal delivery as nulliparous partituents
- Were healthy during the gestation of the first born

Exclusion Criteria

Females who

- Requested **or** was provided systemic or regional analgesia, including inhalation anaesthetics, spinal or epidurals and opioids (any routes) during delivery of their first child
- Reported having no opportunity for labour analgesia for any reason.
- Required assisted vaginal delivery, including use of Ventouse or forceps for their first child
- Had diabetes or hypertension induced by pregnancy of their first born
- Have known neurological (including channelopathies causing congenital insensitivity to pain) or psychiatric impairments

Study B Psychometrics, sensory, pain threshold and tolerance assesments

Inclusion criteria

Females

- who donated DNA in Study A or their corresponding controls

Exclusion criteria

Females who

- are pregnant or breast-feeding
- have any rash, broken skin or skin irregularities where sensory testing is performed
- any underlying medical condition or taking any drug that in the opinion of the investigator will interfere with quantitative sensory testing

Table S1. Eligibility criteria for Study A and Study B. *Related to: STARS Methods, 'Human case ascertainment and recruitment'*

Variable	Test cohort			Control cohort					
	n	mean	SD	n	mean	SD	*P*	CI5	CI95
Questionnaires									
HADS (Anxiety)	39	6.05	2.33	33	6.88	3.57	0.25845	-0.62534	2.28035
HADS (Depression)	39	2.10	1.37	33	2.48	2.18	0.77621	-0.99998	0.99996
PCS (Total)	39	9.56	6.97	33	11.18	7.50	0.41189	-1.99996	5.00002
MHLC (Internal)	39	26.59	3.23	33	26.85	3.23	0.73576	-1.26431	1.78179
MHLC (Chance)	39	17.31	5.40	33	18.48	3.92	0.15776	-0.99993	4.00008
MHLC (Powerful Others)	39	14.44	4.06	33	14.97	4.65	0.60498	-1.51513	2.58273
LOTR (Total)	39	17.46	4.60	33	16.97	4.61	0.65036	-2.99994	1.99996
Computerized cognitive assessments (CANTAB)									
Motor Screening Task									
Mean latency	38#	761.3079	447.9984	30#	687.06	135.79	0.85586	-64.69994	43.80002
Mean error	38#	7.208883	1.562239	30#	7.02	1.84	0.42846	-1.16448	0.50038
Rapid Visual Information Processing (RVP)									
RVP A'	36#	0.930904	0.056894	30#	0.92	0.04	0.16740	-0.04706	0.00919
RVP B'	35#	0.890124	0.333482	29#	0.95	0.05	0.47025	-0.01785	0.03418
Spatial Working Memory									
Strategy	38#	27.97	8.19	30#	30.10	6.01	0.29844	-1.00001	5.00003
Total errors	38#	16.39	15.99	30#	19.67	15.51	0.22973	-2.00006	10.99998
Intra-Extra Dimensional Set Shift									
Total errors (adjusted)	37#	18.73	16.45	30#	19.37	16.92	0.45651	-2.00000	3.99998
Stages completed	37#	8.81	0.57	30#	8.70	0.70	0.41987	-0.00003	0.00004
Total trials (adjusted)	37#	83.89	29.30	30#	84.77	29.12	0.51143	-3.99997	6.99994
One Touch Stockings of Cambridge									
Mean choices to correct	37#	1.09	0.07	30#	1.20	0.23	0.06084	-0.00005	0.10006
Mean latency to correct	37#	9689.43	4320.31	30#	10839.52	3998.01	0.06460	-70.24996	3115.09998

Table S2. Psychometric results for Study B. *Related to: STARS Methods, 'Clinical questionnaires, cognitive and sensory testing & Cambridge Neuropsychological Test Automated Battery (CANTAB)*

HADS, Hospital Anxiety and Depression Scale; PCS, Pain Catastrophising Scale; MHLC, Multi-dimensional Health Locus of Control; Life Orientation Test-Revised (LOTR). n, number of participants; #equipment unavailable/failure; SD, standard deviation; CI5-CI95, 5-95% confidence interval.

Table S3 [Provided as '*Table S3 SNP allele frequency data.xlsx*']

List of all SNPs in discovery cohort that had a cohort allele frequency that deviated from the expected frequencies found in either the 1000 Genomes, European data or the Exome Variant server European data sets. *Related to: Figure 1A.*

For each SNP the following data is shown; its genomic location, number of cases and allele frequency for the rare allele in the research cohort and 1000 Genomes project and Exome Variant Server, p value with Bonferroni correction of deviation from expected, p value with false discovery rate correction of deviation from expected, gene in which the SNP change occurred (when occurring within a gene), effect of SNP rare allele base change and the position in c.DNA (when occurring in cDNA), SNP rare allele amino acid change and position (where occurring in a protein), the SNPs dbsnp nomenclature, the rare allele change Polyphen score and SIFT score.

A Pain threshold	KCNG4+			KCNG4 -			P unadjusted	*P* adjusted*	CI5	CI95
	n	mean	SD	n	mean	SD				
Heat (°C)	3	10.1	5.00	69	14.2	9.10	0.31000	NA	-17.3	9.0
Cold (°C)	3	43.8	3.00	69	43.3	3.20	0.80000	NA	-7.2	8.2
Cuff-pressure (mmHg)	3	196.2	13.80	69	139.7	56.10	0.00290	0.0090	29.7	83.4

B Pain threshold	Test cohort (KCNG4+ individuals excluded)			Control cohort			P unadjusted	*P* adjusted*	CI5	CI95
	n	mean	SD	n	mean	SD				
Cuff-pressure (mmHg)	3	164.2	56.20	33	113.0	9.30	0.00008	0.0005	27.2	75.1

Table S4. *Related to: Table 1*

(A) Effect of the rare allele of *KCNG4* on pain thresholds. *KCNG4+*, individuals who possess the rare allele, *KCNG4-*, controls who do not possess the rare allele; n, number of participants; SD, standard deviation; * Sidak's correction; CI5-CI95, 5-95% confidence interval. **(B)** Comparison of the Test cohort (women who do not possess the rare *KCNG4* allele and did not require analgesic during nulliparous labour) and Control cohort. n, number of participants; SD, standard deviation; * Sidak's correction; CI5-CI95, 5-95% confidence interval.

A	K_V6.4	K_V6.4-Met419
n	8	7
Capacitance (pF)	22.9 ± 1.4	23.2 ± 1.8
Access resistance (MΩ)	8.2 ± 1.1	7.8 ± 0.9
Activation		
$V_{1/2}$ (mV)	-5.4 ± 1.8	-9.8 ± 1.1
k	8.6 ± 1.5	8.9 ± 0.9
Inactivation		
1st component		
$V_{1/2}$ (mV)	-0.8 ± 29.5	-36.2 ± 3.3
k	-46.1 ± 25.6	-63.9 ± 26.5
2nd component		
$V_{1/2}$ (mV)	-60.2 ± 6.6	-33.8 ± 2.1**
k	-29.6 ± 8.1	-26.4 ± 15.6

B	K_V6.4-Met419	K_V6.4	Untransfected
n	10	8	6
RMP (mV)	-50.10 ± 2.05	-47.33 ± 1.14	-46.00 ± 2.14
Capacitance (pF)	41.54 ± 10.17	31.53 ± 3.69	21.55 ± 4.78
Ramp Threshold (pA)	248.60 ± 50.33*	91.56 ± 16.74	112.50 ± 32.51
Number of ramp AP	12.70 ± 3.48	10.22 ± 2.47	15.50 ± 4.79
Step Threshold (pA)	172.00 ± 34.44*	61.11 ± 12.18	88.33 ± 13.76
Amplitude (mV)	75.20 ± 5.20	76.66 ± 6.72	59.87 ± 4.62
HPD (ms)	3.79 ± 0.81	5.69 ± 1.26	3.71 ± 0.62
AHP Duration (ms)	16.48 ± 1.65	31.53 ± 7.35	17.17 ± 3.16
AHP_{50} (ms)	8.52 ± 0.75	10.32 ± 2.15	8.75 ± 1.40
AHP Amplitude (mV)	18.49 ± 1.80	15.92 ± 1.97	17.95 ± 2.90
AP Freq @ 2xThr	6.40 ± 1.17	3.00 ± 0.73	4.33 ± 2.44

Table S5. *Related to: STARS Methods, 'Whole-cell patch-clamp recordings'*

(A) Electrophysiological characteristics of mouse sensory neurons transfected with wild-type K_V6.4 and K_V6.4-Met419. ** $P < 0.01$, mean ± SEM **(B)** Action potential parameters of mouse sensory neurones transfected with wild-type KV6.4 or K_V6.4-Met419 and untransfected cells from current clamp experiments. RMP, resting membrane potential, AP, action potential, HPD, half peak duration, AHP, afterhyperpolarisation duration, Thr,, threshold, Freq., frequency. *P <0.05, mean ± SEM

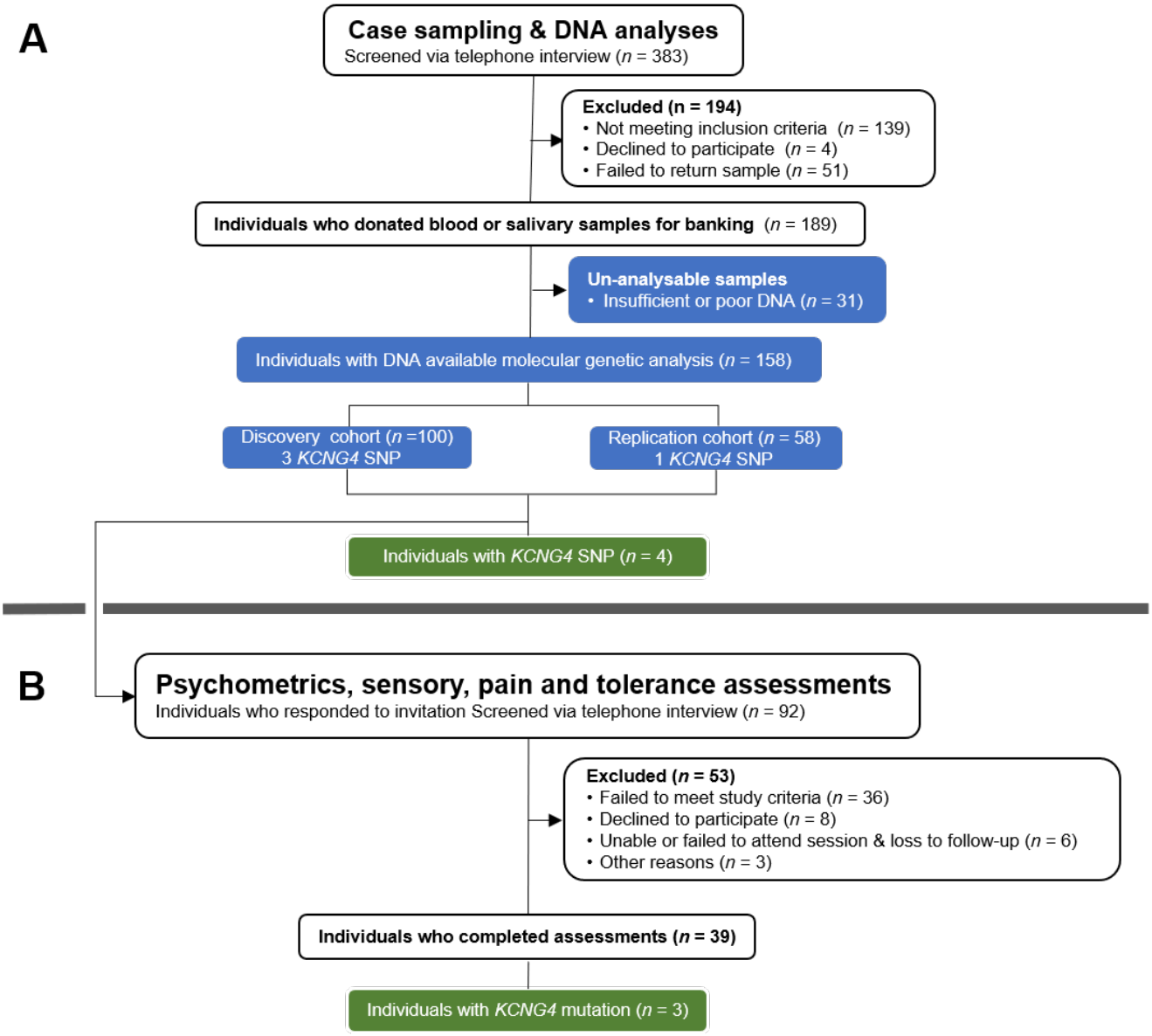

Figure S1 Flow-chart illustrating the recruitment and screening of participants. *Related to STAR Methods, 'Human case ascertainment and recruitment'*

(A) genetic sampling and **(B)** the subset of those participants who underwent psychometric, sensory and pain (threshold and tolerance) assessments. Blue rectangles indicate handling, processing and analyses of DNA samples that were donated by participants. Green rectangles indicated number of individuals assessed or DNA analysed with *KCNG4* mutation. n, number of samples or individuals.

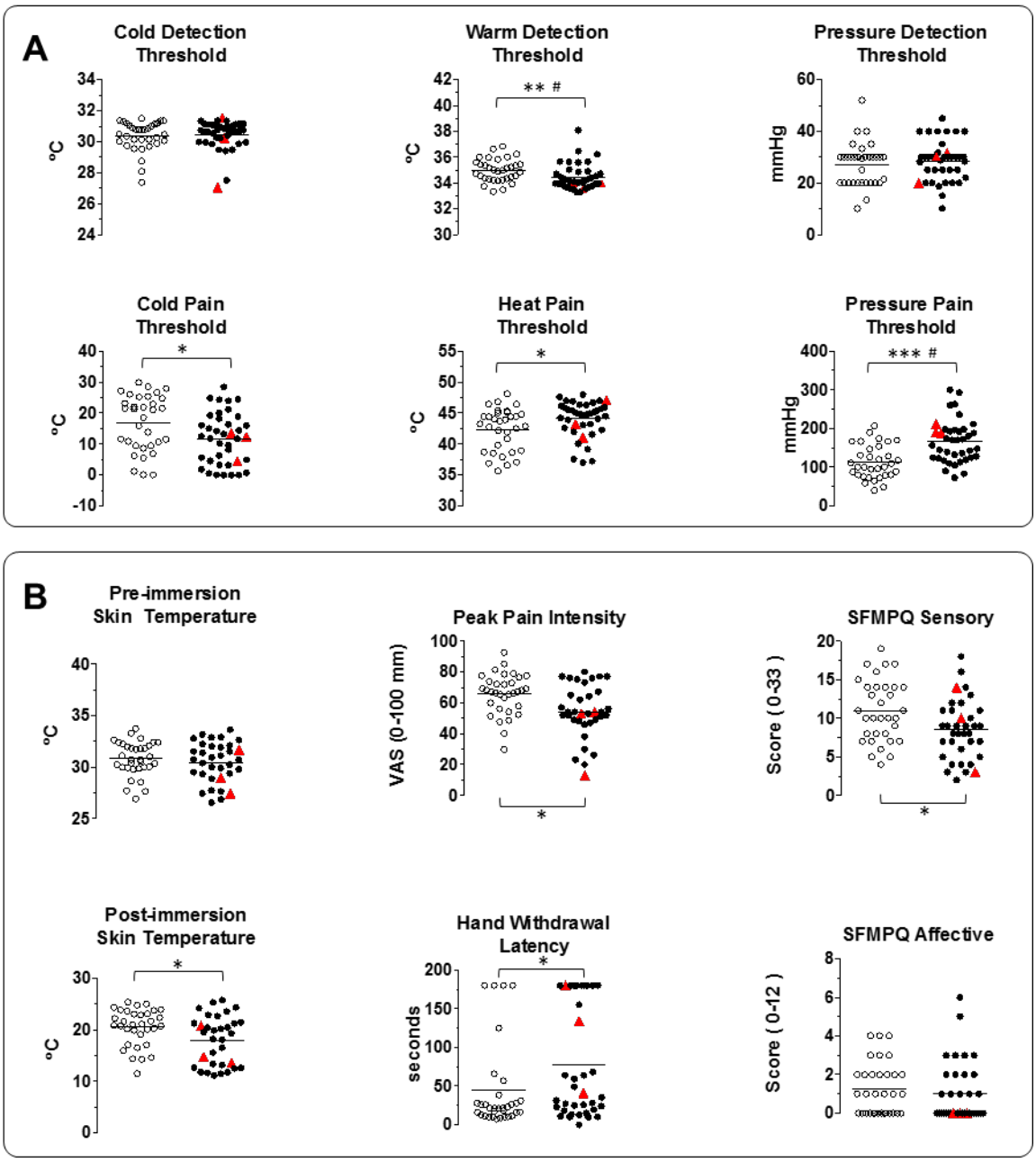

Figure S2 Sensory detection, pain threshold and tolerance assessments. *Related to: Table 1*

(A) Thresholds for sensory detection and pain for heat, cold and cuff pressure. (B) Testing of pain tolerance to hand immersion in cold water. Left-sided graphs: skin temperatures pre- and post-immersion. Middle graphs: withdrawal latency and ratings of peak pain experienced during hand immersion. Bottom graphs: ratings of the sensory and affective qualities of pain experienced with the SFMPQ. Clear circles indicate individuals in control cohort, and filled circles indicate those in the test cohort. The three individuals with KV6.4 p.Val419Met are indicated by red triangles. Horizontal lines represent the mean for each cohort. * P<0.05, ** P<0.01 *** P<0.001; # Sidak adjusted P <0.05

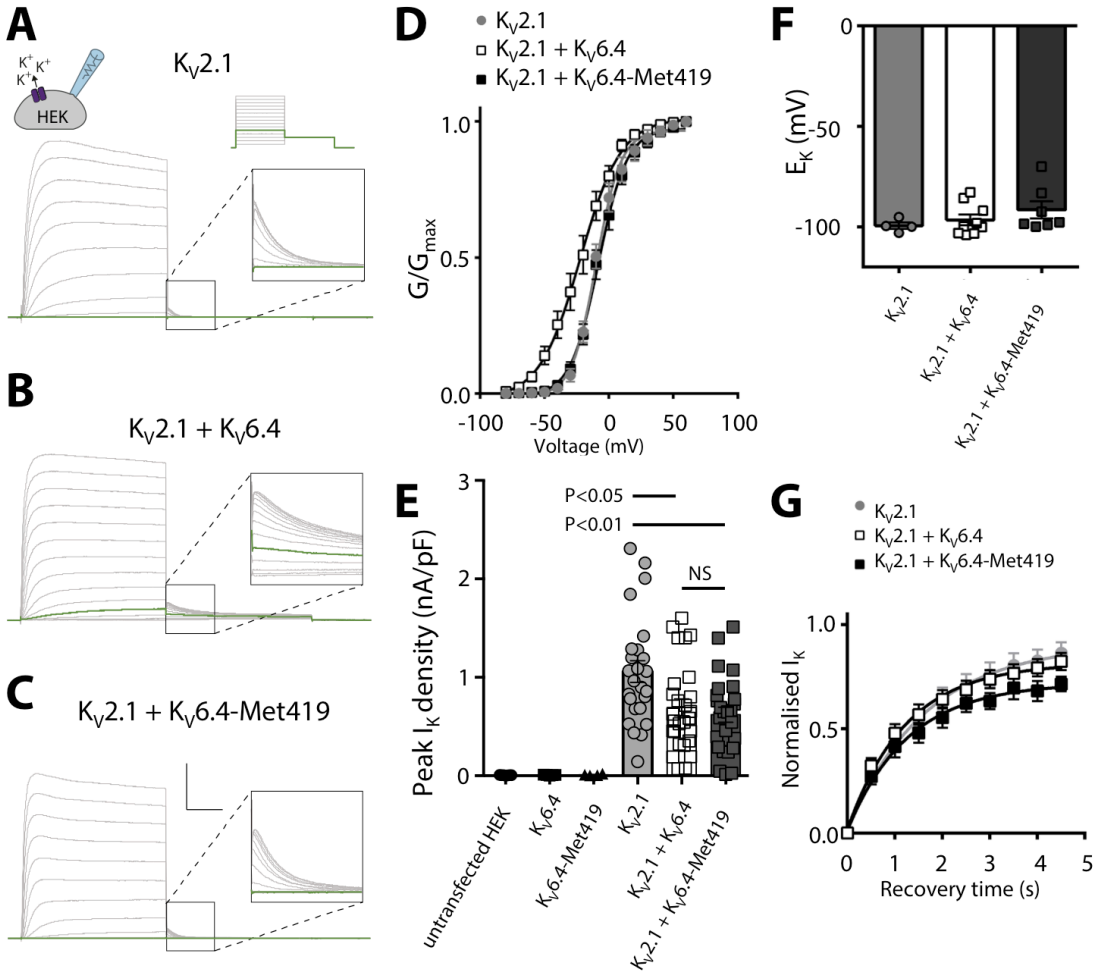

Figure S3 Supporting electrophysiology data for the functional effects of Kv6.4 and Kv6.4-Met419 on Kv2.1 currents in HEK293 cells. Representative current recordings to determine Kv2.1. *Related to: Fig. 1*

(A), Kv2.1/Kv6.4 (B), Kv2.1/Kv6.4-Met419 (C) channel activation properties. The applied voltage protocols are illustrated above the currents shown in (A). Vertical scale bar is 10 nA, horizontal scale bar is 50 ms. Green traces indicate currents recorded during the −40 mV prepulse. D. Voltage-dependence of activation of Kv2.1 (grey filled circles, *n* = 13), Kv2.1/Kv6.4 (open squares, *n* = 14), and Kv2.1/Kv6.4-Met419 (black squares, *n* = 13). The voltage-dependence of activation was determined by normalising tail currents at −60 mV as a function of a prepulse from −80 to +60 mV, in +10 mV increments. Solid lines represent the Boltzmann fitted curves. (E) Peak K^+ current density obtained from +30 mV step of voltage protocol. Bars indicate mean values, error bars indicate SEM. First three groups, *n* = 4-7 from 2 independent experiments, last three groups, *n* = 25-27 from 5 independent experiments. (F) Reversal potential obtained from a linear fit of tail currents from −10 mV to a series of voltage steps from −140 to −50 mV, in +10 mV increments. Bars indicate mean values, error bars indicate SEM, *n* = 4-9. (G) Recovery time from inactivation of Kv2.1 (grey filled circles, *n* = 6), Kv2.1/Kv6.4 (open squares, *n* = 10), and Kv2.1/Kv6.4-Met419 (black squares, *n* = 9). Relative peak current plotted from a 200 ms test pulse to +20 mV at various time intervals following a 5 s prepulse to +20 mV. Solid lines represent exponential fitted curves. Error bars represent SEM

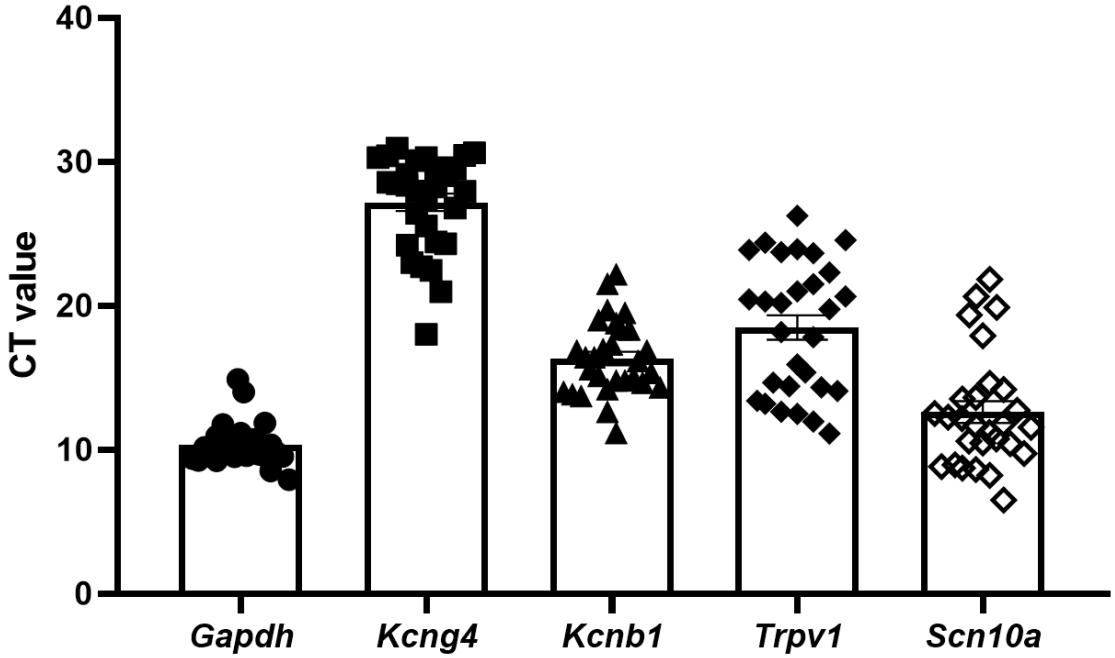

Figure S4 Mean raw cycle threshold (CT) values of *Kcng4*-positive mouse uterus-innervating sensory neurons. *Related to STAR Methods, 'Single-cell qRT-PCR of mouse uterus innervating sensory neurons'*

Data are shown (n=30 cells) for each gene assessed by single cell quantitative PCR analysis. Cells with CT values for specific genes above the quantification threshold of 35 were considered negative and not graphed. Error bars represent SEM.

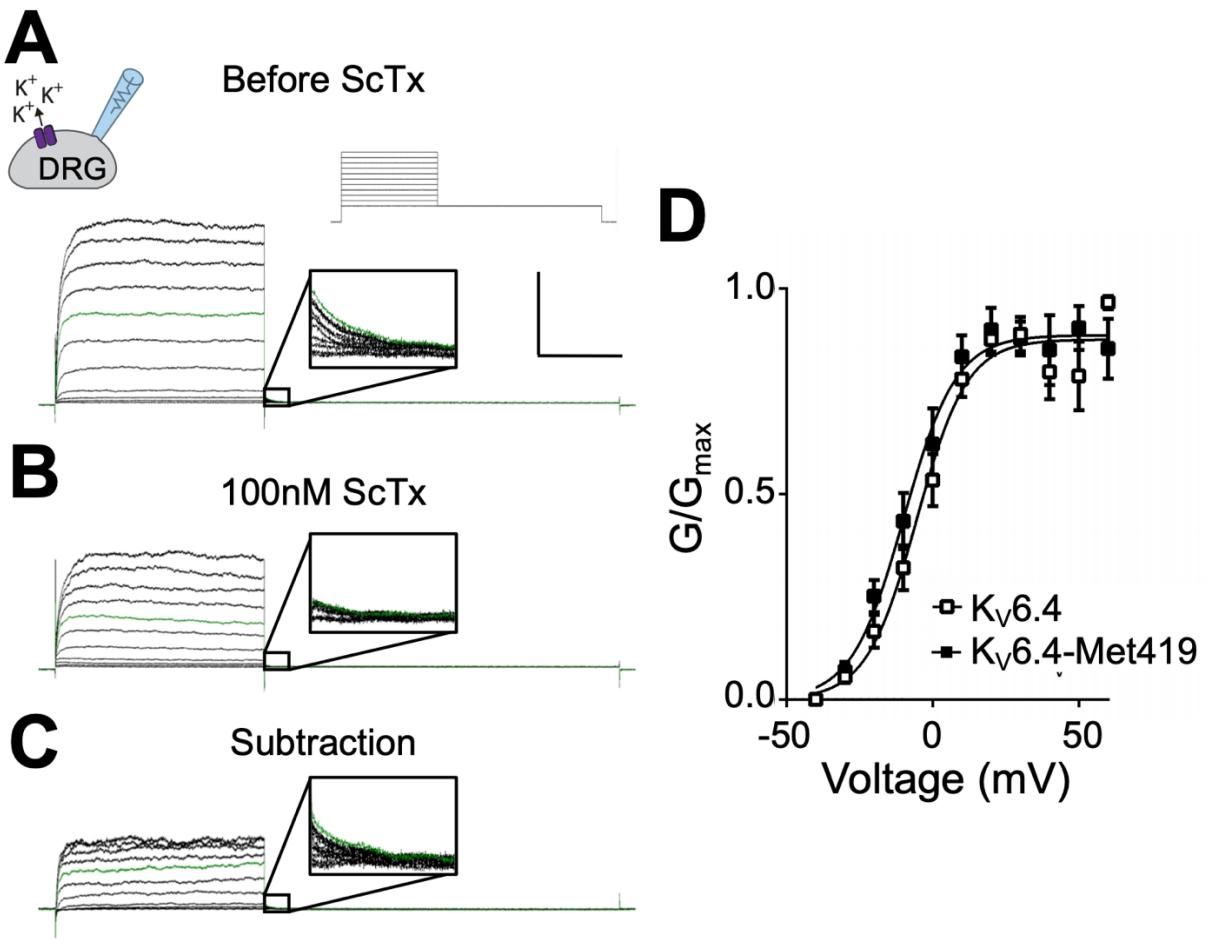

Figure S5 Effect of K_V6.4 and K_V6.4-Met419 on the voltage dependence of activation of the stromatoxin-1-sensitive current in mouse sensory neurons. *Related to STAR Methods: 'Whole-cell patch-clamp recordings'*

(A) Representative I_K recordings produced by *inset* voltage protocol in the absence and presence of 100nM ScTx (B). (C) The ScTx-sensitive I_K is isolated by subtraction of B from A. Expanded tail currents are shown for all three representative traces, each *inset* is 50 ms by 450 pA. The green tracing in A, B and C represent the current at +20 mV. (D) Activation curve of the ScTx-sensitive I_K obtained from mouse sensory neurons transfected with either wild-type K_V6.4 (n = 8) or K_V6.4-Met419 (n = 7). In both cases a Boltzmann function was fit to the data. Error bars represent SEM

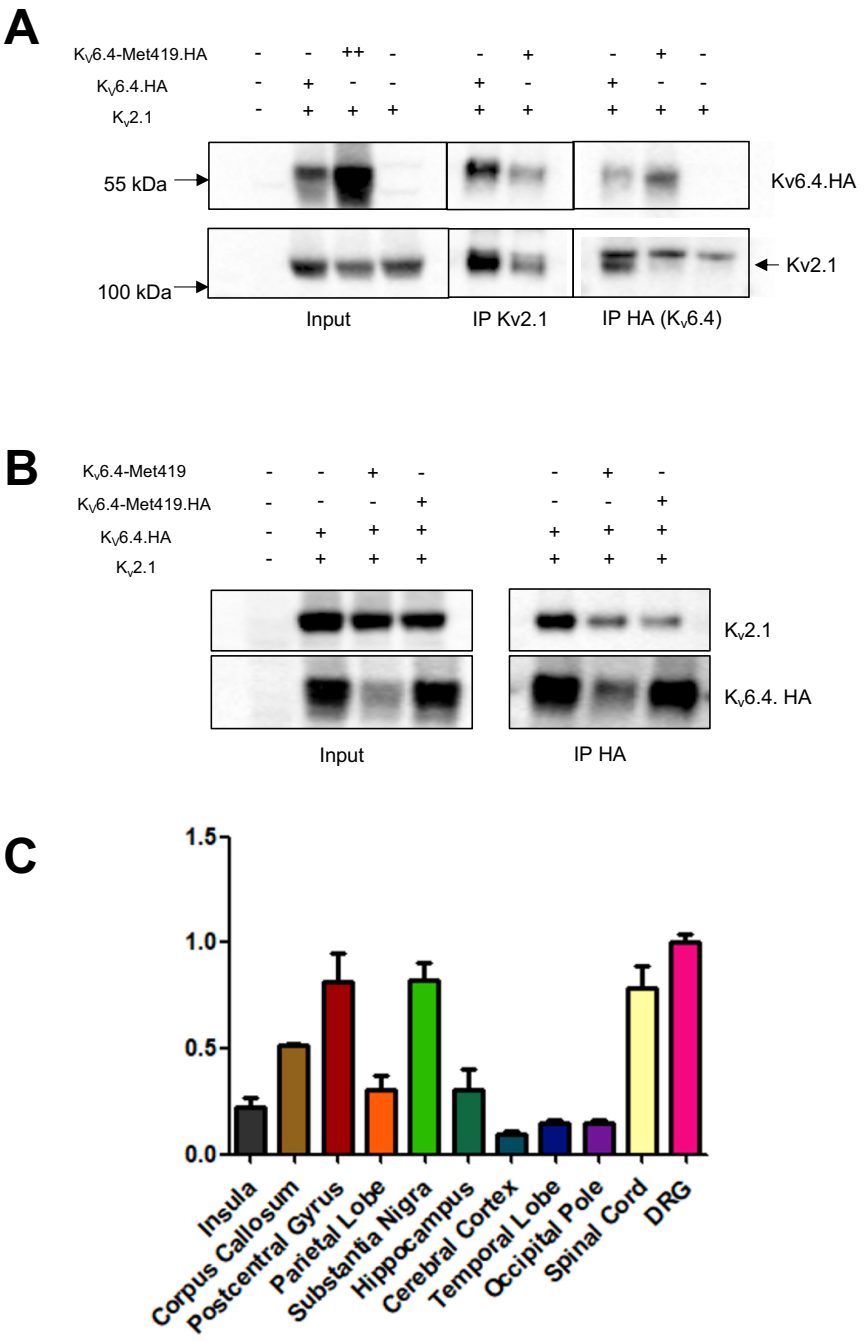

Figure S6. Data supporting lack of heterotetramerisation of Kv6.4-Met419 with Kv2.1 *Related to STAR Methods: 'Co-immunoprecipitation'*

(A) Co-immunoprecipitation experiments showing absence of Kv2.1 binding to Kv6.4-Met419 is not due to Kv6.4-Met419 lack of stability. There is significantly reduced binding of Kv6.4-Met419 to Kv2.1 even when significantly overexpressed compared to Kv6.4. This blot also confirms that HA antibody does not pull down Kv2.1 in the absence of Kv6.4 expression. (B) Co-immunoprecipitation experiment for Kv6.4 and Kv2.1 demonstrating that there is similar reduced binding for Kv6.4 to Kv2.1 in the heterozygous mutant state, whether or not the Kv6.4-Met419 is tagged with HA or not. (C) Expression levels of *KCNG4* in different human brain regions, the spinal cord and DRG (dorsal root ganglion). The graph displays the mean of three mRNA/cDNA conversions, assessed by TaqMan qPCR normalised to a *GAPDH* control and compared with the highest expressing tissue, the dorsal root ganglion (DRG). Error bars represent SEM.

Table S3